universität wien

DIPLOMARBEIT

Titel der Diplomarbeit

A Subcellular Fractionation That Allows The Measurement Of The Proteome And The Metabolome

Verfasser:

Benedict Dirnberger

angestrebter akademischer Grad

Magister der Naturwissenschaften (Mag.rer.nat.)

Wien, im Jänner 2013

Studienkennzahl lt. Studienblatt:	A 441
Studienrichtung lt. Studienblatt:	Diplomstudium Genetik - Mikrobiologie
Betreuerin:	Dipl.-Biol. Dr. Stefanie Wienkoop

“Science is like riding a rollercoaster once you’re up then you are down and when you are down you don’t think you are getting up again”

Professor Kim Nasmyth

Contents

List of Figures

List of Tables

List of Abbreviations

2D- PAGE	Two-dimensional gel electrophoresis
AMDIS	Automated Mass Spectral Deconvolution and Identification System
GC-TSQ-MS	Gas chromatography coupled to triple quadrupole mass spectrometry
LC-TSQ-MS	Liquid chromatography coupled to triple-quadrupole mass spectrometry
LC-Orbitrap-MS	Liquid chromatography coupled to Orbitrap mass spectrometry
NAF	Non- aqueous fractionation
NIST	National institute of standards and technology
MS	Mass spectrometry
MudIT	multidimensional protein identifications technology
rpm	runs per minute
SC	spectral count
SDS- PAGE	sodium dodecyl sulfate polyacrylamide gel electrophoresis
SRM	Selective reaction monitoring
RuBisCO	Ribulose-1,5-bisphosphat-carboxylase/-oxygenase
TAIR	The Arabidopsis Information Resource

1. Introduction

The proteomes of organelles and cellular structures are reduced in their complexity in comparison to highly complex whole cells or tissues. To study the proteome of complex structures in detail such as leaf tissues it is crucial to isolate organelles and cellular structures. The limitation of the detection of low- abundance proteins is caused by the presence of high- abundance protein (Peck, 2005). After translation of mRNA's to protein the maturation of proteins does not stop. Many posttranslational modifications are possible, such as phosphorylation, acylation, ubiquitylation, sumoylation, or proteolytic processing and many more. Most often the low abundance proteins are the ones that underlie a high rate of posttranslational modifications and are important in cell signalling. Therefore, it becomes of special interest to develop strategies to isolate subcellular compartments from complex structures to study the proteome in more detail. The metabolome refers to the complete set of metabolites synthesized in a cell done by the multistep activity of certain enzymes. Metabolic profiles can be detected in combination with different omics approaches such as proteomics (Nadella et al. 2012). Therefore, it was of special interest to establish a combined proteomic and metabolomic technique on sub-cellular level.

1.1. Metabolomics and proteomics in the context of mass spectrometry

The powerful omics technologies including proteomics and metabolomics, today enable an unbiased identification and the study of interactions of molecules in a cell. The term proteome and metabolome represents the total set of proteins or metabolites synthesis in a cell at a certain time. These large- scale analyses of proteins and metabolites are carried out using mass spectrometry. In contrast to the proteome the metabolome has no direct link with the genetic code and metabolites are therefore the product of many concerted actions of enzymatic reactions from a complex network (Saghatelian et al. 2005). Therefore the development of combined proteomic and metabolomic techniques will shed light on cell metabolism and will enhance the new field of system biology.

To analyze proteins in a complex mixture the multidimensional protein identification technology (MudPIT) was developed (Wolters, Washburn, & Yates, 2001). With this method it is possible to define a complex protein mixture in a shotgun approach. This means that proteins are first digested in a solution to receive tryptic fragments of peptides and are analyzed directly without using a 2D-PAGE separation. Therefore shotgun proteomics is a rapid procedure to analyze proteins in a complex mixture (Wienkoop et al. 2004).

State of the art technique to measure the metabolomes is the use of either gas or liquid chromatography coupled with mass spectrometry. It is the goal of metabolomics to measure the complete range of primary and secondary metabolites present in a cell. It is believed that the plant kingdom may contain between 20.000 and 1.000.000 different metabolites and that a single species has a few thousand of them (Obata et al. 2012). In *Arabidopsis thaliana* it is estimated around to 5000 (Saito et al. 2010; Auria et al. 2005). Therefore an important aspect of metabolic regulation is the analysis of compartmentalization of these thousands of different metabolites.

1.2. Subcellular fractionation for metabolomics

It is believed that metabolites are highly compartmentalized in a cell. This is a result of organelle specific metabolite conversion catalysed with many enzymes (Oikawa et al. 2011). A promising approach for studying metabolite compartmentation is the use of non- aqueous fractionation (Gerhardt and Heldt, 1984). The non- aqueous fractionation technique consists of several steps. First the plant material has to be harvested and immediately frozen in liquid nitrogen. The material is then homogenized to a fine powder and for removing the water the powder has to be lyophilized. Then the powder is resuspended in a non- aqueous liquid mixture and ultrasonicated. After a filtration- and a centrifugation step the crude extract is loaded onto a density gradient consisting again of non-aqueous liquid. The gradient is then ultracentrifugated and nine fractions are collected. The fractions are then dried in a desiccator to remove non- aqueous liquid and after drying the fractions the enzyme activity and the metabolites can be measured. Several marker enzymes to define the compartmental boundaries are known from literature (Geigenberger et al. 2011; Tiessen et al. 2012). For each enriched fraction the distribution of the metabolites can be calculated with the data of the marker enzymes using linear regression models (Riens et al. 1991). This calculation gives the proportion of the metabolites in each fraction in the compartments.

1.3. Subcellular fractionation for proteomics

In subcellular proteomics, organelles or cellular compartments are first isolated to enrich them and then analyzed by mass spectrometry. The quality of the proteomic readout of the organelles depends on the detection of the proteins that are present in low abundance compared to high abundance proteins (Lee at al. 2010). The fact that Ribulose-1,5-bisphosphat-carboxylase/-oxygenase (RuBisCO) represents at least 50% of the soluble proteins shows the difficulties of dealing with low abundant proteins as these proteins often play an important role in signal transduction and regulations in the cell (Glinski et al. 2005). This shows the importance of the further development of subcellular fractionation techniques for the research field of proteomics. Classical methods to enrich organelles and cellular structures are subcellular centrifugations. The concept of subcellular fractionation was first developed in rat liver tissue (De Duve et al. 1955). The first procedure in subcellular fractionation for proteomics involves the disruption of the cell. The main liquid methods for separating different cellular compartments are the implementation of density gradients. The density gradient can be divided into continuous- and step gradients. This thesis provides two different methods for the setting up of density gradients. The non- aqueous fractionation is a typical example for a continuous density gradient, since the density of the liquid in the tube is increasing continuously. In the case of a step gradient two or more layers of different densities are layered one above the other. An example for isolating cellular compartments using a step gradient is the use of Percoll gradients. Many standard protocols for isolating cellular compartments based on Percoll gradients have been developed (Daher et al., 2011; Dubinin et al., 2011; Kristian 2010; Eubel et al. 2007; van Wijk et al. 2007).

1.4. Experimental setup

A subcellular fractionation of leaf tissue was performed using non-aqueous fractionation. Therefore two plant model organisms were investigated. From the nine different fractions received from the gradient three aliquots were taken and two different experiments were implemented: an unbiased analysis of the proteome using a LC- orbitrap MS, and an analysis of the metabolome using GC-TSQ-MS. With the resulting data a compartmentation analysis of the distribution of the different metabolites and proteins in three compartments in cell was performed.

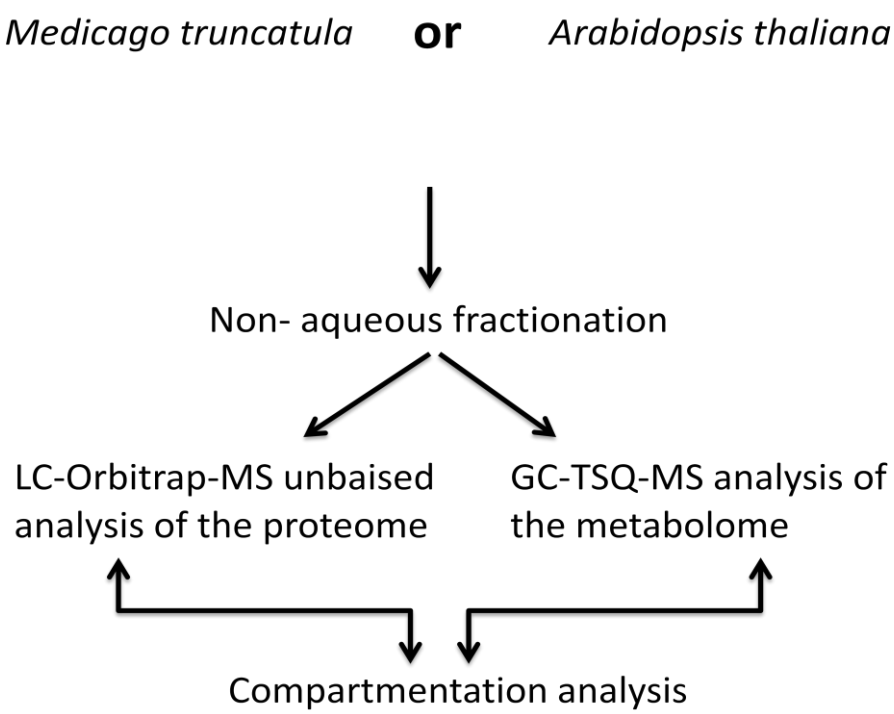

Figure 1.1: Schematic of the experimental setup. Two different experiments were performed and from these data a compartmentation analysis of the different compartments in the cell was made.

1.5. Arabidopsis thaliana and Medicago truncatula as model plants

The most popular model plant is *Arabidopsis thaliana* and was sequenced in the year 2000 (The *Arabidopsis* Genome Iniative. 2000). This plant has a small genome (125 Mb total) and has five chromosomes. The rapid life cycle of six weeks offers scientists to obtain results quickly and easy cultivation of this plant makes it simple to growth this model plant in restricted space in various growth conditions. *Arabidopsis thaliana* is not directly important for major agronomic issues, but offers advantage for basic research like a large number of T- DNA mutant's lines for reverse genetics.

The genome of *Medicago truncatula* is also a small genome in size (~500Mb) and has a diploid genome with 2n= 16 chromosomes (Young et al. 2011). The rapid life cycle, genetically tractable and economic importance of this model plant made *Medicago truncatula* in recent years to an important species in legume science.

1.6. Aim of this work

In summary, this thesis should represent a first investigation of a combined metabolome and proteome fractionation method on sub-cellular level. Therefore NAF was used for the study of subcellular compartments. Nine fractions of NAF were analyzed to determine the distribution of the proteins and the metabolites in the gradient. To measure the proteome a LC- orbitrap mass spectrometer and to specify the metabolome a GC- triple quadrupole mass spectrometer was used. These measurements allow a large scale analysis of the proteomes and metabolomes on subcellular level of a leaf tissue. To compare a continuous gradient with a step gradient a Percoll gradient to isolate chloroplast was established. The proteome was measured using a LC- orbitrap mass spectrometer. Because of the fact that Percoll is an aqueous liquid it is not possible to measure the metabolites in this gradient. The possible measurement of the proteome and the metabolome is therefore a great advantage of NAF.

2. Material and Methods

2.1. Cultivation of *Arabidopsis thaliana* and *Medicago truncatula*

Arabidopsis thaliana and *Medicago truncatula* were cultivated in a glass house (15 h light periode and 9 h dark periode; 25-30 °C day/18-22 °C night) in soil. Leaves of each plant species were harvested in an adult stage (*Arabidopsis thalina:* ~ 4 weeks after germination, *Medicago truncatula:* 8 weeks after germination)

2.2. Non-aqueous fractionation (according to Geigenberger et al. 2011)

The leaf metabolism was stopped as quickly as possible since the turnover rate of metabolites can be extremely fast. Therefore liquid N_2 was used to stop the metabolism. Leaves of both species from similar developmental stages were cut with scissors and collected in a 50 ml falcon tube attached to a liquid N_2 pre- cooled plastic funnel. The falcon tube contained liquid N_2 and was put on ice. After the leaves were collected the liquid N_2 was discarded and the falcon tube was immediately stored in a dewar containing liquid N_2. The frozen leaves were homogenized into a fine powder. Therefore the leaf material was placed into a liquid N_2 pre- cooled steel ball mill containing metal mill balls. The ball mill was then fixed in an oscillating Retsch mill. The material was homogenized at 30 Hz for 15 seconds three times. In this time period the ball mill and the leaf material did not defrost. The homogenized material was transferred again into the 50 ml Falcon tube and was placed into liquid N_2. During freeze-drying the falcon tube with a half open cap was placed into a pre- cooled lyophile (Alpha 2-4, Martin Christ). The material was dried at -18°C at 4 Pa for ~70 h. After 3 days the sublimation stopped and the leaf material was dried. After lyophilisation the Falcon tube with the respective cap was closed as quickly as possible. 80 mg of the dried leaf material was used immediately for fractionation. The remaining material was or could have been stored at -80°C for 3 weeks. Before using the cold stored material the Falcon tubes were put inside a desiccator until the tube reached room temperature and then the tubes were allowed to be opened.

10 ml of tetrachlorethylen/heptanes mixture (v/v 70:30; d = 1,3 g/cm^3) was added to 80 mg of homogenized material in a glass jar. The glass jar was closed and put on ice. Then the suspension was placed under the sonicator. The ultrasonic needle was placed through a hole in the stopper of the glass jar. To avoid overheating during sonication the glass jar was put on ice. The sonication step was repeated for 36 times with 5 seconds of sonication and 15 seconds of pause with strength of 60%. In order to remove particles that are too big, the suspension was filtered through a myo cloth net (30nm in pore size) into a 50 ml Falcon tube. This step was made inside a desiccator. The filter was washed with 10 ml ice cold heptane. The desiccator was closed and waited until the suspension was filtered. The Falcon tube was centrifugated at 4000 rpm for 10 min at 4°C. After the tubes reached room temperature the supernatant was discarded and the pellet was resuspended in 1,5 ml of tetrachlorethylen/heptanes mixture (70:30). After resuspending the pellet 1 ml of the crude extract was loaded onto the gradient. The gradient was then centrifugated for 3 h by 4°C at 30.000 rpm in an ultracentrifuge (Beckman instruments *SW4ITI* 6 bucket rotor). After centrifugation 9 fractions of 1 ml

were collected from the top to the bottom and pipetted into a 2 ml microtube. Three aliquots from the 9 fractions each 300 µl were transferred into new 2 ml microtubes. To each microtube 1 ml of n-heptan was added. The three aliquots of the 9 fractions were then centrifugated for 3 min by 13000 g. 1ml of the supernatant was discarded and the three aliquots of the 9 fractions and the remaining crude extract were dried in a desiccator.

2.3. Calculation of the distribution of the analytes in the gradient (according to Riens et al. 1991)

Three aliquots from nine fractions received from the gradient were collected and different experiments were performed. With the data of the different experiments a compartmentation analysis of the distribution of metabolites and proteins in different compartments in a cell were performed. The compartmentations analyses of the metabolites were performed using a system of linear equations.

$$a_{11}x_1 + a_{12}x_2 + a_{13}x_3 = z_1$$

$$a_{21}x_1 + a_{22}x_2 + a_{23}x_3 = z_2$$

$$a_{31}x_1 + a_{32}x_2 + a_{33}x_3 = z_3$$

- The coefficient “a” stands for the distribution of the marker enzymes in the gradient
- The variable “x” stands for the distribution of the metabolites in the gradient
- The solution set “z” stands for the peak area of the metabolites resulting from the chromatogram

The system contains three equations resulting from the three compartments: chloroplast, cytosol/ mitochondria and vacuoles. In the case of nine fractions the best solution of the linear equations system can be described through the method of least squares. This method proves an approximate solution of an overdetermined system. As a result an analytical solution is replaced through an optimization process and the percentage of the metabolites in the three compartments can be determined.

2.4. Extraction for protein analysis (according to Staudinger et al. 2012)

For protein extraction the total fractions stored in the desiccator were homogenized in 500 µl of urea or tris buffer. After a centrifugation step by 10000 g for 10 min at 4°C the supernatant was transferred into a falcon tube. 5ml of ice-cold aceton, 0,5% mercaptoethanol was added. The falcon tubes were then stored over night at –20°C for precipitation. Then the falcon tubes were centrifugated by 4000 g for 15 min at 4°C. After the supernatant was discarded the pellet was resuspended in 2 ml of ice-cold methanol and 0,5% mercaptoenthanol. The falcon tube was then centrifugated by 4000 g for 10 min at 4°C. The pellet was then dried under a hood. The dried pellet was dissolved in 10 µl of urea or tris buffer. This step was repeated until the pellet was completely dissolved. The protein concentration was then determined via Bradford protein assay.

Table 2.1: 1.Extraction of protein for non-aqueous fractionation

Component	Final concentration
Tris-HCl	50 mM
DTT	1 mM
$MgCl_2$	5 mM

Table 2.2: 2.Extraction of protein for non-aqueous fractionation

Component	Final concentration
HEPES, pH 7.8	500 mM
Urea	8 M

To enhance the yield of extracted proteins steel balls were transferred into the micro tubes and the tube was shortly vortex. This procedure was repeated for several times and at each time the micro tube was put on ice. The dried fraction could be dissolved better in buffer containing Tris-HCl and so this extraction was our first choice for extracting proteins.

Table 2.3: Bradford solution (according to Bradford et al. 1976)

Component	final concentration
ddH_2O	225 ml
Ethanol	15 ml
Phosphor acid 85%	30 ml
Coomassie brilliant blue g-250	150 mg

The determination of unknown protein concentration via Bradford reagent relies on the fact that the sulfonate groups of the dye Coomassie Brilliant Blue G250 binds to positive charge residues of proteins. As a result the absorption maximum of the dye defers from 465 nm to 595 nm. As a result of the high percent of the phosphoric acid concentration the proteins become denaturated and thereby the binding of the dye to the residues of the polypeptides is enhanced.

2.5. Phenol extraction (according to Carpentier et al. 2005)

The dried pellet was dissolved in 50 µl extraction buffer. For a better dissolution the pellet was heated for 2.5 min at 95°C. Then 200 µl of 1.4 M sucrose and 300 µl of phenol was added to the reaction tube and after vortex the reaction tubes were incubated at room temperature for 10 min. After several minutes two phases were visible. The reaction tubes were centrifugated for 5 min at full speed. The upper phase was transferred into a new tube. For recovery more protein 100 µl phenol was added to the old reaction tube. Then it was centrifugated again for 5 min at full speed and the supernatants were combined. For precipitation the 2 ml reaction tube was filled up with 0.1 M Ammonium acetate in methanol. The proteins were precipitated over night at -20°C. To obtain the protein pellet the reaction tube was centrifugated for 10 min at full speed. The supernatant was discarded and the pellet was washed with 0.1 M ammonium acetate in methanol and then in acetone. The pellet was dried for 5 min at room temperature and was dissolved in 30 µl of 8 M urea buffer.

2.6. Isolation of chloroplast using Percoll (according to Daher et al. 2011)

Leaves of *Medicago truncatula* were harvested into a 50 ml falcon tube and put on ice. They were then transferred into a 100 ml beaker and the buffer for homogenization was added. Three times of the volume homogenized buffer was added to the leaves. They were then homogenized three times two seconds by 50% of speed using a mixer with a sharp razor blade. All steps were performed on ice. The time and the speed of mixing are very important because it is easily possible that the chloroplasts burst. After filtering the homogenate through a myo cloth net to a 10 ml backman tube the resulting filtrate was centrifugated at 200 g for 1 min by 4°C. The supernatant was transferred into a new tube and centrifugated at 3500 g for 3 min by 4°C. At this step the pellet has to be without starch. This would be an indicator that the chloroplasts had burst. The supernatant was discarded and the pellet was resuspended in 100 µl of wash medium. The resuspended pellet was loaded on top of the Percoll gradient. The gradient was then centrifugated at 3750 g for 10 min by 4°C using a swing-out-rotor. After centrifugation the isolated chloroplasts were collected from the 50%/80% Percoll interphase and transferred into a new 1,5 ml safe lock microtube and 200 µl of wash medium was added. This step is important because without diluting the Percoll it is not possible to receive a pellet with chloroplast. After the centrifugation step at 1200 g for 3 min by 4°C the supernatant was removed and the intact chloroplasts were frozen at -20°C to break them up. To prove the isolation of the chloroplast a sodium dodecyl sulfate polyacrylamide gel electrophoresis (SDS-PAGE) was performed. The chloroplasts were first resuspended in 200 µl of tris buffer. This step was performed

with the help of steel balls to break further up the chloroplasts. The proteins were precipitated over night in ice cold aceton/0,5% mercaptoethanol. After a centrifugation and a washing step in ice- cold methanol/0,5% mercaptoethanol the precipitated proteins were dissolved in 500 µl of tris buffer. The Protein concentration was determined using Bradford protein assay (Bradford et al. 1976). For the control SDS-PAGE 10 µg of protein were loaded onto the gel.

Table 2.4: Extraction buffer for isolation of chloroplast

Component	Final concentration
Tricine-NaOH, pH 7.9	50 mM
Sorbitol	330 mM
EDTA	1 mM
$MgCl_2$	1 mM
BSA	0,1%

For extracting chloroplast from a complex cell mixture it is important that the chloroplasts are intact when they are isolated. An indication for burst chloroplasts is white starch in the pellet after centrifugation. This leads to a furthermore disruption of the chloroplasts.

Table 2.5: Wash medium for isolation of chloroplast

Component	Final concentration
Tricine-NaOH, pH 7.9	50 mM
Sorbitol	330 mM
Percoll	10% v/v

Table 2.6: 80% Percoll solution

Component	Final concentration
Percoll	3,2 ml
EDTA	250 mM
Hepes	1 M
Sorbitol	0,24 g
ddH_2O	ad 4 ml

Table 2.7: 50% Percoll solution

Component	Final concentration
Percoll	2 ml
EDTA	250 mM
Hepes	1 M
Sorbitol	0,24 g
ddH_2O	ad 4 ml

2.7. Protein digestion

2.7.1. In solution digestion (according to Staudinger et al. 2012)

For digesting the extracted proteins were dissolved with urea buffer or tris buffer and digestion was performed with the sequencing grade endoproteinase Lys-C (1:100, vol/vol, Roche, Mannheim, Germany) for 5h 30 min. These enzymes cut specificly at lysine or arginine residue. The samples were diluted with trypsin buffer. The second digestion step was carried out using Poroszyme immobilized trypsin beads (8 h at 37°C).

Table 2.8: Trypsin buffer for digesting proteins

Component	Final concentration
Acetonitrile	10%
ammonium bicarbonate	50 mM
$CaCl_2$	2 mM
adH_2O	4.2 ml

2.7.2. In gel digestion (according to Shevchenko et al. 2007)

The band on the gel was cut with a razor into two parts. Each part was sliced further into smaller pieces. The gel pieces of each part were transferred into a 1.5 ml reaction tube. 100 µl of 100 mM ammonium bicarbonate/50% acetonitrile was transferred into the tube. They were incubated at 30°C for 30 min on the thermomixer. The supernatant was removed. This step was repeated. 100 µl of acetonitrile was pipetted into the reaction tube. After 5 min the gel pieces were white and this was a sign that the gel pieces were dry. After drying the gel pieces 50 µl of 20 mM dithiothreitol/ 100 mM ammonium bicarbonate were transferred into the reaction tube after an incubation step at 30°C for 30 min on the thermomixer. The supernatant was removed. This step was necessary for reducing disulfide bond. 70 µl 50 mM Iodacetamide / 100 mM ammonium bicarbonate was added into the tubes. Again the reaction tubes were incubated for 30 min and this time the thermomixer was covered with aluminium foil since Iodacetamide is photosensitive. The supernatant was discarded and 100 µl 25 mM ammonium bicarbonate was transferred into the reaction tube and incubated for 15 min at 30°C on a thermomixer. The supernatant was again removed and this step was repeated. 100 µl of 25 mM ammonium bicarbonate/ 50% acetonitrile was transferred into the tube and incubated on a termomixer for 15 min. The supernatant was removed and then 50 µl of acetonitril was put into the tube, incubated at room temperature for 5 min and the supernatant was removed. The small gel pieces were dried in a speed vac. For disgesting the protein in the gel trypsin was added (12.5 ng/µl and o/n). To recover the solution with the peptides the tubes were spinned down and the liquid was put into a new low binding tube. To recover all peptides from the gel 40 µl of 20% acetonitril/ 1% formic acid was transferred into the remaining tubes. They were incubated at room temperature for 5 min and sonicated for 3 min in a sonication bath. The supernatant was combined into the low binding tube. This step was repeated with 40 µl of 50% acetonitril/ 1% formic acid and 40 µl 90% / 1% formic acid. The combined liquid of peptides was dried in the speed vac.

Table 2.9: Ingredients for 11 % polyacrylamide gel

Ingredient	Resolving gel	Stacking gel
30 % acrylamide	4 ml	0.73 ml
Tris-HCl 1.5 M	2.5 ml	
Tris-HCl 0.5 M		2.5 ml
10% SDS	100 µl	100 µl
10% ammoniumpersulfate	50 µl	55 µl
TEMED	5 µl	3 µl
ddH_2O	ad 10 ml	ad 5.5 ml

Proteins can be separated in an electric field according to their molecular weight. Therefore the residues of the proteins have to be charged and denaturated. This is made with the help of a SDS containing Lämmli sample buffer for 5 min at 99°C. After this step the proteins are denaturated and charged and can be loaded onto the gel. For running the gel a mini VE vertical electrophoresis system was used at 120 V and in room temperature.

- 4 x Lämmli sample buffer (LSB): 40% glycerol, 8% SDS,0,25 M Tris-HCl pH 6.8, 20% 2-mercaptoethanol 0.004% Bromophenol blue
- 10 x Electrophoresis buffer: 30 g Tris, 144 g Glycine, 10 g SDS, pH 8.3 dH_2O ad 500 ml

Coomassie staining

For visualization of proteins on a polyacrylamide gel a coomassie dye in acid is used. In this thesis a self-mixed stain as described below was used for the staining. For destaining, the gel was transferred into a destaining solution lacking Coomassie dye for three times. To enhance the destaining reaction the gel was then transferred into water over night.

- Staining/Destaining solution: 40% Metanol, 10% Acetic acid plus 0.1% CoomassieR-250 only for staining

2.8. Desalting peptides

2.8.1. Desalting with 96 –well solid phase extraction plate

First the membrane was equilibrated, once with 250 µl of methanol and then two times with 250 µl of milli Q water. The samples were centrifugated before loading on the column. Then the columns were washed twice with milli Q water and the peptides were eluated twice with methanol. The samples were splitt into two 0.5 ml low binding tubes and dried in a speed- vac. The samples were stored at -20°C until the measurement.

2.8.2. Desalting through stage-tips (Ishihama et al. 2006)

Three tiny pieces of C18 column were transferred into a 200 µl yellow tip and then the tip was transferred into a 2 ml micro-tube with a hole in the lid. The membrane was then equilibrated once with 100 µl of methanol/ 0.1% formic acid and then two times with 100 µl mili Q water/ 0.1% formic acid. Then the samples were loaded onto the column. The flowthrough was run again through the membrane for a better yield of proteins. The column was then twice washed with 100 µl of milli Q water/ 0.1% formic acid. The elution step was performed two times with 100 µl of Methanol/ 0.1% formic acid. The eluate was collected in low binding tubes and dried in a speed-vac.

2.9. NanoESI LC-MS/MS

The dried peptides were dissolved in 5% acetonitrile (ACN), 0.1% formic acid (FA). The dissolved peptides were loaded on a column with a concentration of 0,5 µg. The column was linked to a UHPLC system and to an Orbitrap LTQ XL mass spectrometer (Thermo Electron, Bremen, Germany). Different time gradients were used from 90% solvent A (0.1% formic acid in water) to 80% solvent B (80% acetonitrile, 0.1% formic acid in water) with 500 nL/min to elute the peptides.

2.10. Metabolite extraction (Weckwerth et al. 2004)

The dried pellets of the nine fractions and the crude extraction were homogenized in 1 ml extraction buffer with the help of a mill containing steel balls for 10 seconds by 30 rpm and incubated for 8 min on ice. After the centrifugation step for 4 min by 14000 g the supernatant was transferred into a 2 ml microtube containing 500 µl milli Q water. The remaining pellet was used for extracting the lipids and the lipophilic phase of the metabolites. After vortex and a centrifugation step for 4 min by 14000 g the supernatant was divided into two 1,5 ml microtubes. An internal standard 10 µl of 0.1 g sorbitol was added and the samples were dried in the speed- vac. The dried samples were then stored at -20°C. To analyze the lipids and the lipophilic phase of the metabolites the remaining pellet of the metabolite was extracted. Therefore 1 ml of extraction buffer was added to the pellet. After vortex the samples were incubated at room temperature for 3 h. After a centrifugation step of 4 min by 10.000 g the supernatant was transferred into a 2 ml microtube containing 400 µl milli Q water. At this point two phases were visible. The upper phase contains the lipophilic part of the metabolites and the lower one contains the lipid phase. The samples were centrifugated again for 2 min by 10.000 g and the two phases were divided into 1,5 ml microtubes. An internal standard 10 µl of 0.1 g sorbitol was added for the hydrophilic part and for the lipids C17:0 was used. The samples were dried in a speed- vac and the dried samples were then stored at -20°C.

Table 2.10: Extraction buffer for metabolites

Component	Final concentration
MeOH	2,5 ml
$CHCl_3$	1 ml
H_2O	0,5 ml

2.11. Derivatization of metabolites

The samples stored at -20°C were brought to room temperature and 20 µl of methoximation mixture was added to the dried samples to dissolve them. After the samples were shaken in the thermo mixer for 90 min at 30°C 80 µl of silylation solution was added. The samples were shaken again for 30 min at 37°C. After a centrifugation step for 2 min by 10000 g the supernatant was transferred into a glass vial with a micro insert.

2.12. Esterification of lipids

The dried pellet was resuspended in 292 µl tert- butylmethylether and 5µl tri-methylsulfoniumhydroxid. The samples were incubated for 30 min at room temperature before they were measured on the GC-TSQ-MS.

Table 2.11: Methoximation mixture

Component	Final concentration
Methoxyaminhydrochlorid	40 mg
Pyridine	1 ml

Table 2.12: Silylation solution

Component	Final concentration
N-Methyl-N-(trimethylsilyl) trifluoroacetamide	1 ml
Alkane	60 µl

3. Results

For the assessment of the combined technique that allows the measurement of the metabolome and the proteome under subcellular level the NAF technique was used (Stitt et al. 1989). To compare the strength of this technique with another isolation protocol a step gradient consisting of several layers of Percoll was implemented. Over all, this part of the thesis deals with a first summary giving new insights into a fractionations method that allows the combined measurement of the metabolome and the proteome using the leaf tissue of two plant model organisms *Arabidopsis thaliana* and *Medicago truncatula.*

3.1. Aspects of the Non-aqueous fractionation technique

It turned out that normalized spectral counts are good indicators for the marker enzyme activity in the fraction. Therefore three sets of three marker enzymes (showing in figure 3.4) for each compartment were normalized and used for the calculation. Using different marker enzymes for the compartmentation analysis of different metabolites is a possibility to proof the robustness of the calculation. The best way to analyze the distribution of the proteins found in the large scale proteomic experiment is to look at the individual spectral counts in each fraction. Spectral counts are discrete numbers of identified peptides found in a protein sequence.
The NAF method provides water free environment of lyophilized tissue and separation of particles in a density gradient. After the homogenized tissue is freeze dried and re- suspended in a water- free tetrachlorethylene/*n*-heptane mixture [density 1,3 g/cm^3] the particle size and clustering have to become less than 30 µm. Therefore the samples have to be ultrasound sonicated. The particle size and clustering is an important aspect in the separation of each fraction using a linear gradient consisting of *n*-heptane and tetrachlorethylene as non- aqueous solvents. The collected fractions have to be diluted using n- heptane and divided into aliquots for further analysis. The individual fractions consist of different cellular compartments. Throughout the first five fractions the content of the chloroplast continually regresses. The middle fractions of the gradient contain the cytosolic compartment. It is discussed that the mitochondrial compartment is not considered to be unambiguously separated from the cytosol (Klie et al. 2011). The last fractions contain the vacuoles. These distributions of the three compartments are normally visible in a nine fraction gradient. The use of citrate synthase, as a marker for the mitochondrial compartment, for a six fraction gradient was detected throughout the gradient (Krueger et al., 2011). Therefore the choices of the number of analyzing fractions influence the results.

3.2. Metabolomic analyses

To analyse the subcellular distribution of the metabolome in leaves, the NAF method was selected. Metabolites were analyzed using a gas chromatography coupled to triple quadrupole mass spectrometer. The table 3.1 shows the 78 metabolites found in *Arabidopsis thaliana*, identified with the NIST and AMDIS library and clustered into five chemicals families. To determine the percentage of the metabolites in the three compartments the linear equation system was used. This thesis provides a few examples of calculated percentages of the metabolites in the different compartments. The calculation was performed with a set of three different marker enzymes shown in figure 3.2.

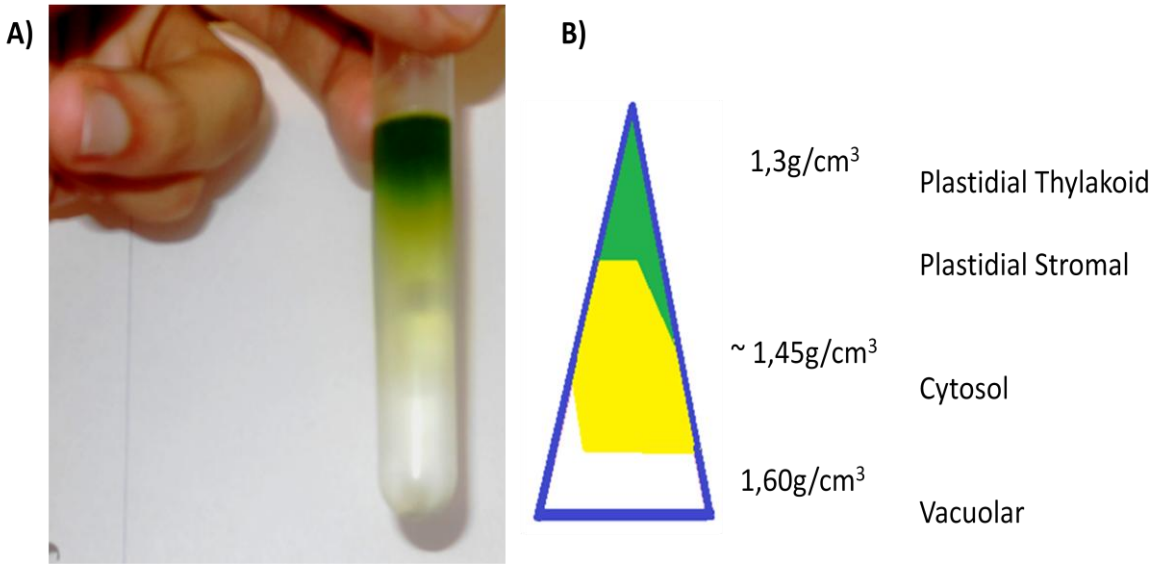

Figure 3.1. A NAF gradient after ultracentrifugation and the distribution of the cellular compartments in the gradient. A NAF gradient is shown in A). This gradient is a typical example of a continuous density gradient .The progression of the sub- fractionation is visible from dark green to transparent. The rising density of the gradient is shown in B). The gradient has a density from 1.3g /cm^3 to 1.6 g/cm^3. At the density around 1.3 g/cm^3 the fractions of the chloroplasts are visible. The cytosolic fractions are around 1.45g/cm^3. The vacuolar fractions are around 1.60g/cm^3.

Table 3.1: List of all Metabolites found in *Arabidopsis thaliana* leaves. The metabolites were grouped into chemicals families: Organic acids, Amino acids & Derivates, Sugars & Sugar alcohols, Fatty acids, Phenolics & Cyclitols. In total 78 different metabolites were identified.

Organic acids	Amino acids & Derivates	Sugars & Sugar alcohols	Fatty acids	Phenolics & Cyclitols
1.Malic acid	21.Serine	33.Fructose	66.2-Propenoic acid	76.Shikimic acid
2.Threonic acid	22.Pyroglutamic acid	34.Glucose	67.7,10,13 - Hexadecatrienoic acid, methyl ester	77.Myo Inositol
3.Succinic acid	23.Alanine	35.Sorbitol	68.Hexadecanoic acid methyl ester	78.Inositol
4.Glyceric acid	24.Threonine	36.Mannitol	69. 7,10,13- Hexadecatrienoic acid, methyl ester	
5.Succinic acid	25.D-Proline	37.Sucrose	70.Propionate	
6.Fumaric acid	26.Glycine	38.Glycerol	71.Octadecanoic acid, methyl ester	
7.Lactic acid	27.L-serine	39.D-(-) Fructose	72.4- Aminobutyric acid	
8.Glutamic acid	28.L-Threonine	40.Glucose methoxyamine	73.Linoleic acid	
9.Citric acid	29.Glutamine	41.Melibiolse	74.Erythronic acid	
10.Glycerol	30.L-Aparagine	42.Sorbose methoxyamine	75.Lyxonic acid	
11.Urea	31.Leucine	43.Galactinol		
12.Oxalic acid	32.Homoserine	44.Melibiose		
13.Ascorbic acid		45.Maltose		
14.Valeric acid		46.Raffanose		
15.Folic acid		47.Arabitol (pentaacetat)		
16.Arginiosuccinic acid		48.Melezitose		
17.Riboflavin		49.Riboluse		
18.Piperidincarboxylic acid		50.Erythritol		
19.Butanoic acid		51.Galactose methoxyamine		
20.Pipecolinic acid		52.Xylose		
		53.Tagatose		
		54.Psicose		
		55.Lyxose		
		56.Mannose		
		57.Talose		
		58.Gulose		
		59.Idose		
		60.Manitol		
		61.Ribose		
		62.Raffinose		
		63.Trehalose		
		64.Kestose		
		65.Arabinose		

For this calculation the peak area of the metabolites and the normalized spectral counts of the marker enzymes were used. As already mentioned the main focus of this thesis was to link the non-aqueous fractionation to large scale proteomics. Time limitation and long waiting times for measurement slots caused the performance of less measurement than hoped for concerning the metabolites. For a correct statement of the distribution of all metabolites found in the experiment it would be necessary to perform the measurement several times to obtain trustworthy data. It is of no

use to calculate the percentage of metabolites of *Medicago truncatula*, as we had not enough repetitions of measured data. It is also not possible to compare the data from *Medicago truncatula* with other published data, as they do not yet exist. Therefore only for a few metabolites concerning *Arabidopsis thaliana* a compartmentation analysis was calculated and compared with data that were already published:

The synthesis of proline is carried out in the chloroplasts and in the cytosol of the mesophyll cells (Lehmann et al. 2011). Recent investigations to determine the percentage of proline in cells of *Arabidopsis thaliana* leaves using NAF showed that this amino acid is dominantly localized in the chloroplasts to 67 ± 6% (Krueger et al. 2011). For this calculation several different markers, as mentioned further on, were used. In figure 3.2 A) the average concentration of proline in the chloroplast results in about 70%. For our calculation we used novel markers listed in figure 3.4 and to integrate the peak area we used the m/z value of 142 and the retention time of 15.63 min.

Threonate is the salt of threonic acid. This acid is a derivate from ascorbic acid and the synthesis of ascorbic acid takes place in plastids (Ilarslan et al. 1997). Recent studies showed a possible role of ascorbic acid signalling during the interoganelle interaction between chloroplast and mitochondria through the cytosol and the peroxisome as a process known as photorespiration (Talla et al. 2011). Krueger and colleagues showed in an analysis of threonate in the cellular compartments in *Arabidopsis thaliana* that threonate is enriched in the chloroplasts (Krueger et al. 2011). They used glyceraldehyde 3-phosphate dehydrogenase as a chloroplastic, UDP-glucose pyrophosphorylase as a cytosolic, citrate synthase as a mitochondria and mannosidase as a marker for the vacuoles.

We used three sets of different marker enzymes showing in figure 3.4: I.Marker: pyrophosphorylase 6, UDP-Glucose pyrophosphrylase 1, vacuolar ATP synthase subunit E1. II.Marker: thylakoid lumen protein, glycerophodiester phosphodiesterase, peroxidase CB. III.Marker: photosystem I light harvesting complex gene 1, cold-regulated 47, vacuolar ATP synthase subunit CB.

Figure 3.2 B) shows the different distribution of the percentage of threonic acid in the specific cellular compartments in leaf tissues. It is visible that threonic acid is enriched in the chloroplasts and the calculation is stable by the use of our set of three different marker enzymes. For the calculation of the peak area of threonic acid the area was integrated using the m/z value of 292 and the retention time of 21.73 min.

A) **B)**

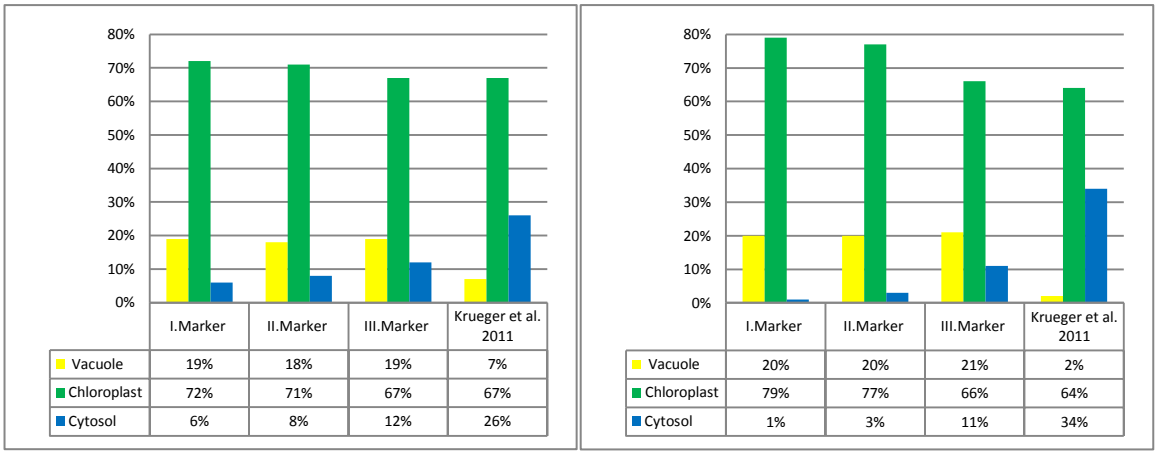

Figure 3.2: Two examples for different metabolites that are enriched in the chloroplasts. One can see that in A) proline and in B) threonic acid is situated in the chloroplasts. The calculation was performed three times with different sets of marker enzymes. The fact that these two metabolites are enriched in the chloroplasts corresponds to the findings of Krueger and colleagues (Kruger et al. 2011). I.Marker: pyrophosphorylase 6, UDP-Glucose pyrophosphrylase 1, vacuolar ATP synthase subunit E1. II.Marker: thylakoid lumen protein, glycerophodiester phosphodiesterase, peroxidase CB. III.Marker: photosystem I light harvesting complex gene 1, cold-regulated 47, vacuolar ATP synthase subunit CB

The lipids of the nine fractions were analysed using a GC- TSQ – mass Spectrometer. For calculation of the distribution of the lipids in the gradient the peak areas were normalized to the dry weight and to the internal standard (Heptadecanoic acid). After normalizing the data one could see two clear distributions of lipids. Only fatty acids from chloroplast membranes had a significant distribution and the others had a ubiquitous distribution in the nine fractions. The linolenic acid is an unsaturated fatty acid that is present in the thylakoid membrane of chloroplast (Siegenthaler et al. 1976). Another specific lipid of *Arabidopsis thaliana* chloroplast is the hexadeca 7,10,13-trienoic acid (16:3$\Delta^{7,10,13}$). The 16:3$\Delta^{7,10,13}$ is the most abundant fatty acid in the thylakoid membrane of *Arabidopsis thaliana* (Heilmann et al. 2004). These two lipids had a specific distribution in the first four fractions. The figure 3.3 shows a continuously decreasing concentration of 16:3$\Delta^{7,10,13}$ and linolenic acid in the first four fractions. The 16:3$\Delta^{7,10,13}$ is a specific *Arabidopsis thaliana* chloroplast lipid and was missing in the chromatogram of the *Medicago truncatula*, showing that this lipid is a specific lipid in the membrane system of chloroplast in *Arabidopsis thaliana.*

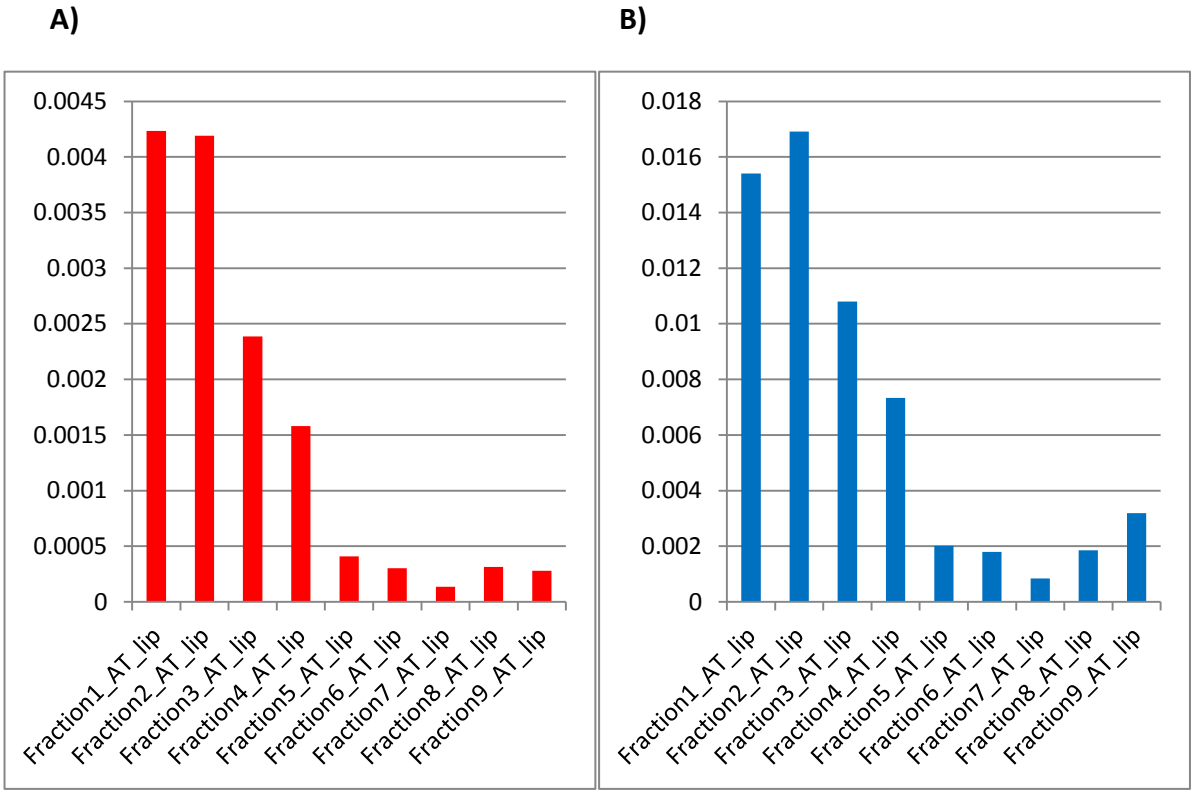

Figure 3.3. The distribution of the A) 16:3 B) 18:3 lipids in the nine fractions. These two lipids are components of the chloroplast. The concentrations of these two lipids are decreasing at the first four fractions. This shows that these lipids are localized in the membrane system of chloroplast. In the fractions five to nine of these lipids are reduced, showing the continuous decreasing of the chloroplast in the nine fractions.

3.3. Proteomic analyses of non- aqueous fractionation density gradients

To analyze the subcellular distribution of the proteome in leaves, the NAF method was selected. The proteins were analyzed with a liquid chromatography coupled to orbitrap mass spectrometer. For this approach proteins were extracted from the nine fractions resulting from the NAF gradient. Each fraction was analyzed using mass spectrometry. The experiment was repeated four times with four gradients. With each measurement the number of identified proteins increased as a consequence of improvement of the extraction methods. The MS/MS spectra were searched against a genomic database (*Medicago truncatula* Gene Index, release 10.0 or *Arabidopsis thaliana* tair, release 10.0) using SEQUEST linked to the MS software Proteome Discoverer 1.3. This algorithm correlates uninterpreted tandem mass spectra of peptides with amino acids sequences from protein databases (Eng et al. 1994). The filters in the Proteome Discoverer 1.3 were set to "medium peptide confidence" and "two different peptides per protein".
In the first experiment a total number of 188 (in *Medicago truncatula*), in the second 428 (in *Arabidopsis thaliana*) and in the third 528 (in *Arabidopsis thaliana*) protein groups were identified in the nine fractions showing in table 3.2. Different methods were applied to extract proteins from the nine fractions. In the case of the first gradient an 8M urea buffer was used for extracting the proteins. To extract the second and the third gradient a tris buffer was used. The protein concentration was determined via Bradford protein assay (Bradford et al. 1976). The proteins were digested in solution using LysC and Trypsin beads. A fourth gradient was extracted using phenol as extraction method. After this extraction procedure the samples were loaded onto a SDS PAGE and the proteins were separated according to their molecular weight. After the proteins entered the running gel for 1 cm the run was stopped and the protein band was cut into two pieces. The proteins were then digested using trypsin and analyzed using mass spectrometry. The in- gel digestion failed and therefore no proteins were identified in this procedure.
For analyzing the distribution of the proteins over the nine Fractions the different spectral counts of each fraction were used. It turned out that the value of the spectral counts is a good indicator for the distribution of each single protein over the gradient showing in table A.1. and A.2. With the values of the normalized spectral counts it is easy to search for marker enzymes that are located in the specific compartment.

Table 3.2: The identified proteins of the nine non- aqueous fractionation experiment. The experiment was repeated three times and for each fraction the number of identified proteins is listed. Through an improvement in the extraction method of the fractions the total number of identified protein groups in the nine fractions increased to 528.

1.Fraction	209	1.Fraction	193	1.Fraction	78
2.Fraction	269	2.Fraction	196	2.Fraction	140
3.Fraction	276	3.Fraction	195	3.Fraction	103
4.Fraction	293	4.Fraction	171	4.Fraction	29
5.Fraction	326	5.Fraction	270	5.Fraction	39
6.Fraction	346	6.Fraction		6.Fraction	33
7.Fraction	239	7.Fraction	207	7.Fraction	119
8.Fraction	230	8.Fraction	149	8.Fraction	28
9.Fraction	203	9.Fraction	72	9.Fraction	47
Arabidopsis thaliana		*Arabidopsis thaliana*		*Medicago truncatula*	
Total: 528		Total: 428		Total: 188	
3.Experiment		2.Experiment		1.Experiment	

A)

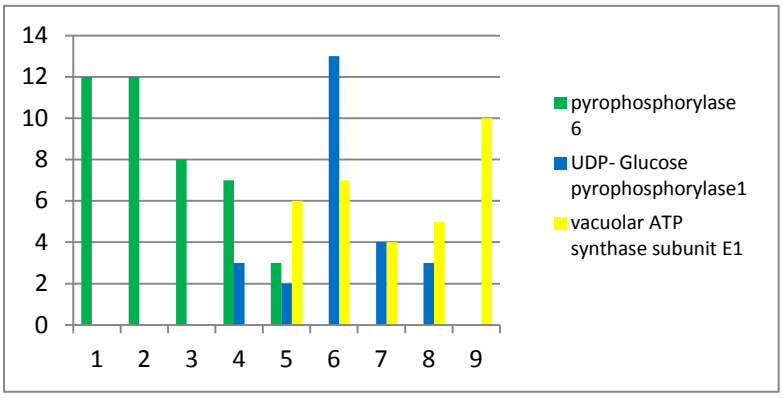

B)

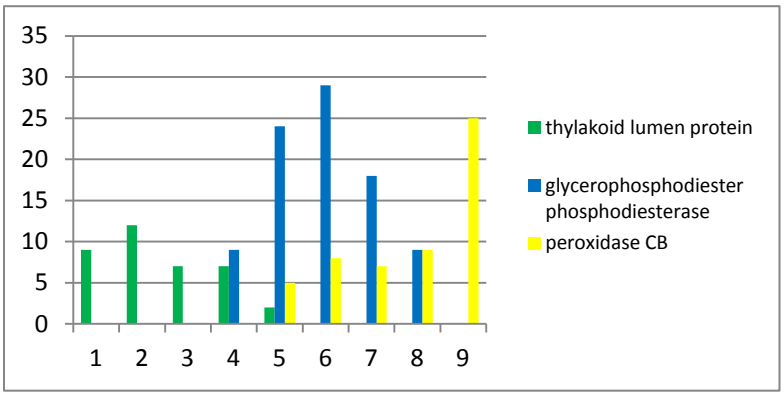

C)

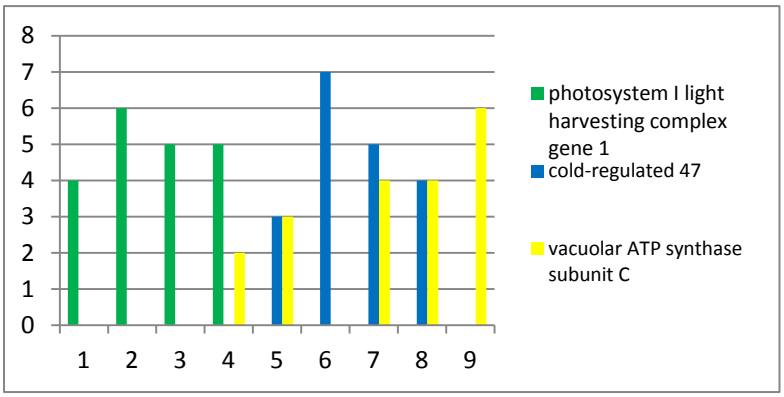

Figure 3.4. Examples of a set novel marker proteins for the three different subcellular compartments of *Arabidopsis thaliana*. In case of A) pyrophosphorylase 6 serves as a marker protein for the chloroplast- compartment. UDP-Glucose pyrophosphorylase 1 serves as a marker protein for the cytosolic compartment and vacuolar ATP synthase subunit E1 serves as a marker protein for the vacuolar compartment. A clear distribution of the three markers is visible. In the first five fractions the content of the chloroplastic marker continuously regresses. Then the cytoplasmatic marker reaches its maximum at fraction 6 and secedes. The vacuolar marker reaches then its maximum at fraction 9. In B) a similar scenario as in A) is shown. In this case a thylakoid lumen protein represents the chloroplast marker protein and the glycerophosphodiester phosphodiesterase stands for the cytoplasmic marker. As vacuolar marker the peroxidase CB is shown. C) The Photosystem I light harvesting complex gene 1 represents the chloroplastic marker, the cold- regulated 47 protein the cytosolic marker, and the vacuolar ATP synthase subunit C the vacuole marker.

3.4. Subcellular distribution of high abundance proteins

It seems obvious that for instance proteins from the photosystem and the calvin cycle are relatively high in comparison with other proteins such as regulatory proteins. The reason is that the photosystem is vital for surviving and this explains the high abundancy of these proteins in the cell. In figure 3.5 chloroplast proteins with high spectral counts (≥ 30) are displayed. All of these proteins show a distribution. One can see that these proteins are localized in the first fractions of the gradient. It is crucial to normalize the data to allow an equalisation of all spectral counts and therefore to obtain a reliable view of the distributions of all proteins. Without normalized data the chloroplast proteins would shift the distribution.

A)

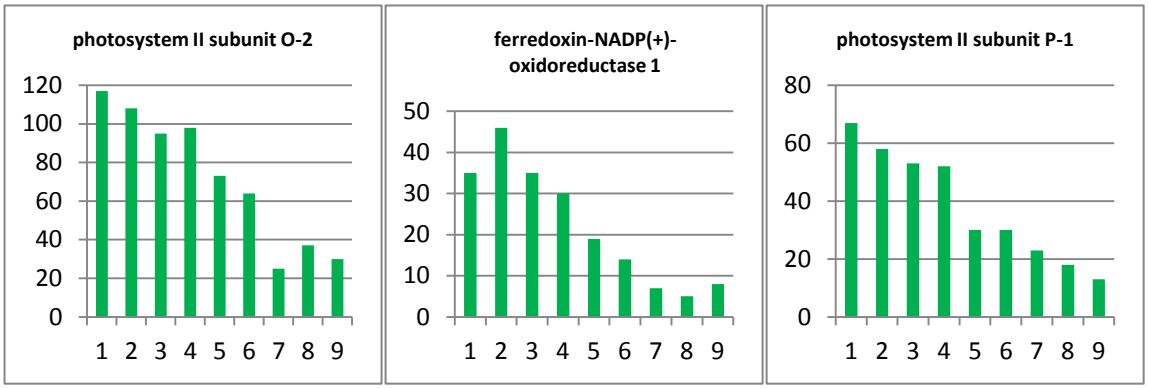

B)

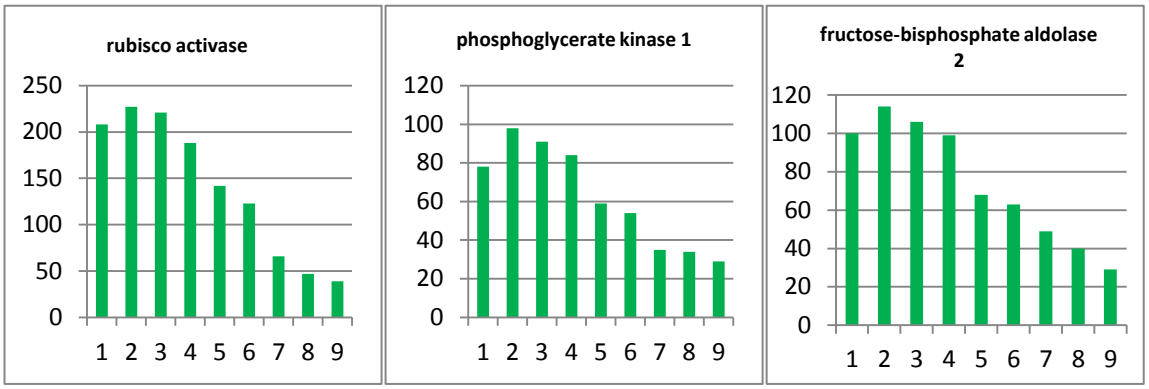

Figure 3.5.High abundance proteins with highest spectral counts in chloroplast fractions. In A) three examples that are functionally categorized to the photosystem II. In B) proteins calvin cycle.

For determining the distribution of the chloroplast ATP synthase the normalized spectral counts of several subunits were used (AT4G04640; AT4G32260; AT4G32260; ATCG00480; ATCG00120; ATCG00470; AT4G09650). The vacuolar ATP synthase is distributed in the last fraction of the gradient. For this approach the normalized spectral count of several subunits of the vacuolar ATP synthase was used (AT1G78900; AT4G11150; AT1G12840; AT1G76030).

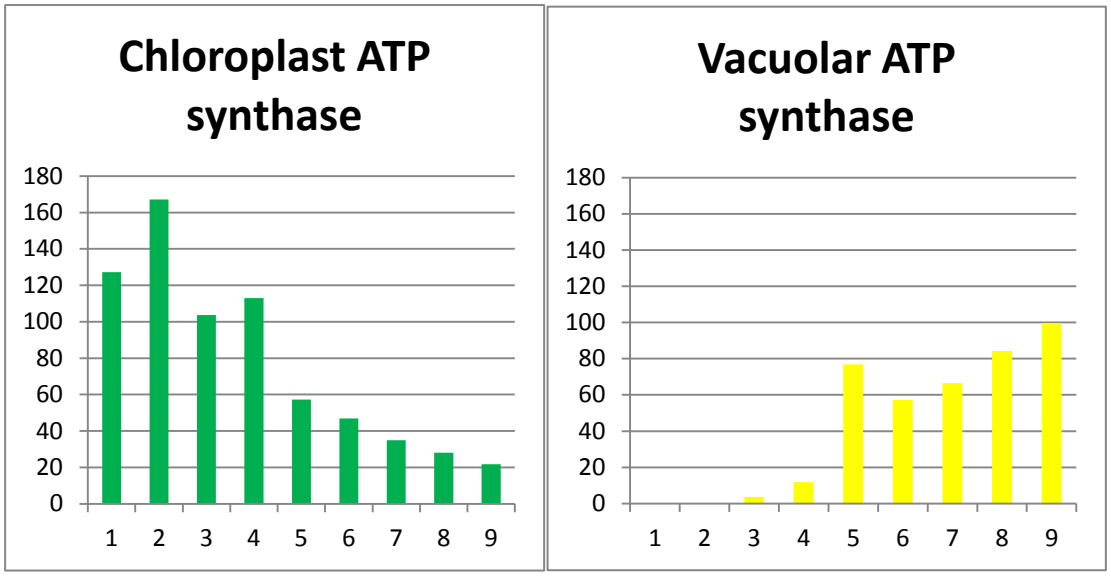

Figure 3.6. The distribution of two different ATP. Chloroplastic ATP synthase can be separated from the vacuolar ATP synthase. The spectral counts of different subunits were used to analyze the distribution.

It was not possible to determine the distribution of mitochondrial ATP synthase since only two mitochondrial subunits were found. The “ATP synthase alpha/beta family protein” (AT5G08670) was found as a possible mitochondrial ATP synthase subunit protein since the spectral counts were larger at the fraction four to six. This could be a sign that the mitochondria are located in the cytosolic fraction of the gradient.

3.5. Proteomic analyses of Percoll density gradients

To compare the NAF method as a continuous density gradient with a step density gradient Percoll was used. Percoll step density gradients were developed for isolating cellular compartments and studying the proteome and therefore many standard protocols were established (Daher et al., 2011; Dubinin et al., 2011; Kristian 2010; Eubel et al. 2007; van Wijk et al. 2007). For isolating chloroplast from *Medicago truncatula* different protocols were used (Daher et al. 2011, van Wijk et al. 2007). After separating the chloroplast and extracting the proteins 10 µg of proteins were loaded onto an 11% SDS PAGE. After staining the proteins on the gel the two subunits of RuBisCO became visible. The proteins were then digested in a solution using LysC and Trypsin beads. The chloroplast proteins were then analyzed using a LC- Orbi- Trap. A total number of 38 different proteins could be identified showing in table A.3.

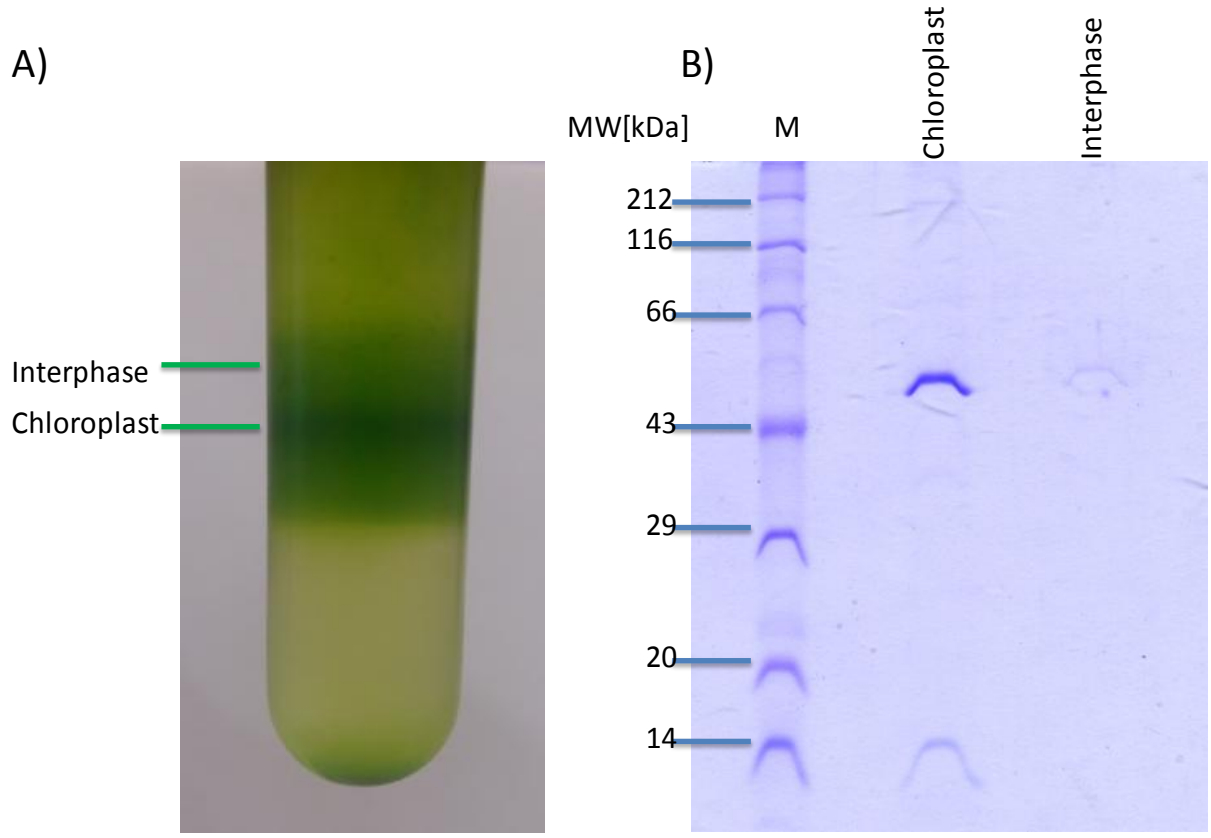

Figure 3.5. The isolation of chloroplast using Percoll. A) In between of the two Percoll density phases (80% and 50%) the dark green insulated chloroplast is visible. B) 10 µg of extracted proteins were loaded onto an 11% SDS-PAGE. The band of the interphase was weaker than that of the chloroplast. The large subunit is at 55 kDa of RuBisCO and the small subunit is at 15 kDa are shown. M Marker Roti®- Mark STANDARD.

4. Discussion

4.1. Metabolomic analyses using non- aqueous fractionation

After analyzing the 9 fractions resulting from NAF 78 different metabolites showing in table 3.1 were found. This result was then compared with other published data to this topic: In other studies that used NAF for analyzing the metabolites in the three cellular compartments in leaves 93 different metabolites were found in *Glycine max* (Benkeblia et al. 2007) and 203 were identified in *Arabidopsis thaliana* (Krueger et al. 2011).

4.2. The strength of the protein separation using non-aqueous fractionation

An entire overview of the protein separation can be best shown using a hierarchical clustering. This was performed with the normalized spectral counts (PSM) of the 528 proteins found in the nine fractions in *Arabidopsis thaliana*. For this reason PageMan was used. PageMan (Usadel et al. 2006) and MapMan (Usadel et al. 2005) is an efficient software tool to evaluate a multiparallel experiment with datasets resulting from different time points. To read the hierarchical clustering sowing in figure 4.1. one has to act as follows:

- Each column represents the normalized spectral counts (PSM) of each fraction.
- The first row of each section (PS, major CHO metabolism,….) is a summary of several individual rows.
- Each individual row in a section represents the distribution of a protein in the nine fractions.

A few examples regarding the localization of proteins shown in figure 4.1 are described in more detail:
The first section analyses the photosystem (PS). The summary of the “PS” shows a clear distribution of chloroplast protein. The dark blue colour in the first four columns (PSM1-PSM4) indicates the presence of chloroplast proteins. Next to them the red colour columns represent the absence of chloroplast proteins. In the last three columns the colour turns from light red to light blue. This shows that certain proteins of certain rows in the section of the photosystem are present also in these columns. A typical example is the distribution of the photorespiration system. The blue colour row called “PS.photorespiration” is not only localized in the first columns but also in the middle and in the last columns. In higher plants, this pathway is localized in three different cellular compartments and contains at least eight core and several auxiliary enzymes (Bauwe et al. 2012). This distribution is the reason for the light blue colour in the last columns.
In the section “glycolysis” it appears that this metabolic pathway is localized in columns six to eight. This shows that this process takes place in the cytosol. An unexpected discovery was the finding of the existence of glycolysis in the plastids (ap Rees, 1987). In the row called “plastid glycolysis” a dark

blue colour is visible in the first two columns showing that this process takes place in the chloroplasts.
The tricarboxylic acid cycle (TCA) is present in the plant mitochondria. In the summary row of the section of “TCA / org. transformation” the blue colour is mainly present in the middle columns showing that mitochondrial respiration is located in the cytoplasm.
Nitrogen is an important source of all organisms and plants usually assimilate nitrogen as nitrate (NO_3^-) and nitrate is then converted to nitrite (NO_2^-) with the cytoplasmic enzyme nitrate reductase. The nitrate assimilation pathway consists of a two step reaction and thereby nitrate is converted to ammonium. This reaction takes place in the stroma of the chloroplasts or in nonphotosynthetic tissues such as roots and is catalysed by the enzyme nitrite reductase (Kherraz et al. 2011). The row called “N-metabolism.nitrite metabolism.nitrite reductase” at the section “N-metabolism” shows that in column two the nitrite assimilation pathway is active. This explains the location of this enzyme in the chloroplast.
In plants the synthesis of tetrapyrrole molecules occurs in the chloroplast, but their cofactors are widespread in the cell and they are transported to the individual compartments (Mochizuki et al. 2010). The summary row of the section “tetrapyrrole” shows a distribution of the synthesis of tetrapyrrole molecules in chloroplast.
Mereschkowsky postulated in the year 1905 that plastids are reduced ‘‘foreign microorganisms’’ and that these microorganisms became endosymbionts of the cell during an early phase of cell evolution (Mereschkowsky, 1905). Microorganisms such as *Cyanobacteria* have prokaryotic ribosomes. In the section “protein” at the row called “protein.synthesis.ribosomal protein.prokaryotic” a distribution of prokaryotic ribosomes is visible. In the following rows further subunits show the same pattern indicating that these proteins are localized in the chloroplasts.
All of a sudden the pattern changes and eukaryotic ribosomes are concentrated in the middle showing that they are localized in the cytosol. These are mainly located in the fraction five to eight.
ATP synthases are enzymes that are located in the membrane system of several compartments. They catalyze the synthesis of ATP from adenosine diphosphate (ADP) and inorganic phosphate (Pi) using an electrochemical potential of protons across the membrane. In plants several locations for the ATP synthases are known such as chloroplast thylakoid membranes, mitochondrial inner membranes or vacuole membranes. The chloroplast ATP synthase consist of two parts. One part is embedded in the thylakoid membrane and the second part is located in the stroma of the chloroplast.
The vacuolar ATP synthase is important for the survival of a plant and is involved in the transport of metabolites, carbohydrates, amino acids, salts across the membrane of the central vacuole. This enzyme acts in several cellular processes such as cell expansion or stress adaptation (Kluge et al. 2003).The physiological consequences of this ATP synthase is the acidification of the vacuole and in consequence of this acidification it is discussed that it facilitates the cell expansion by generating turgor pressure. Another function of vacuolar ATP synthase is the adaptation to salt stress (Padmanaban et al. 2004). In addition to the localization of the vacuolar ATP synthase in the membrane system of the vacuoles some others localisations have been described. The ATP synthase was found in the Golgi apparatus (Matsuoka et al., 1997), endoplasmic reticulum (Herman et al., 1994) and in the plasma membrane (Dietz et al., 2001). In the section transport it is visible that V-ATPasen is distributed in the last columns, showing that these groups of proteins are located in the last fractions of the gradient.

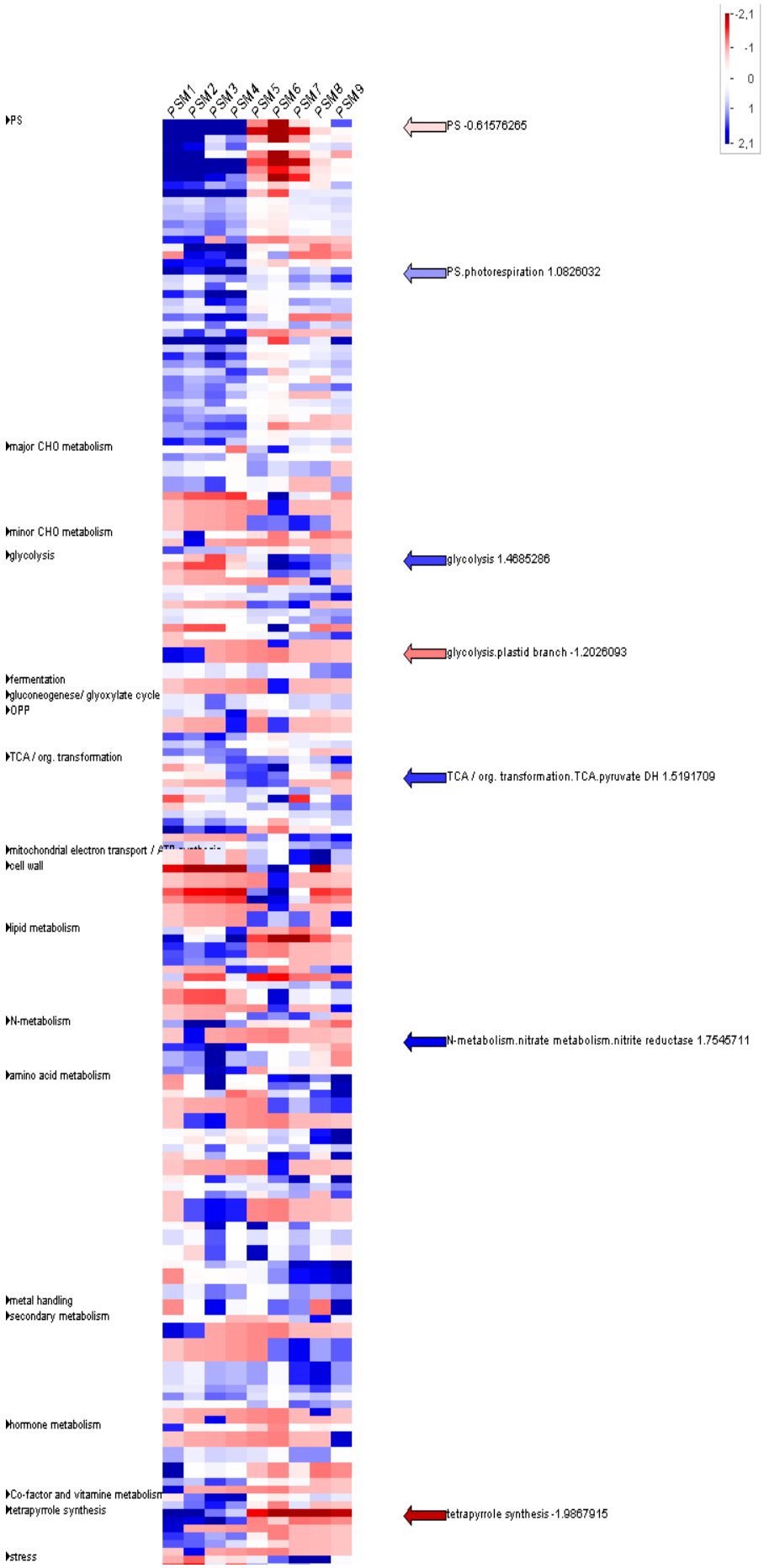
PSM1
PSM2
PSM3
PSM4
PSM5
PSM6
PSM7
PSM8
PSM9
-2,1
-1
0
1
2,1
PS
major CHO metabolism
minor CHO metabolism
glycolysis
fermentation
gluconeogenese/ glyoxylate cycle
OPP
TCA / org. transformation
mitochondrial electron transport /
cell wall
lipid metabolism
N-metabolism
amino acid metabolism
metal handling
secondary metabolism
hormone metabolism
Co-factor and vitamine metabolism
tetrapyrrole synthesis
stress
PS -0.61576265
PS.photorespiration 1.0826032
glycolysis 1.4685286
glycolysis.plastid branch -1.2026093
TCA / org. transformation.TCA.pyruvate DH 1.5191709
N-metabolism.nitrate metabolism.nitrite reductase 1.7545711
tetrapyrrole synthesis -1.9867915

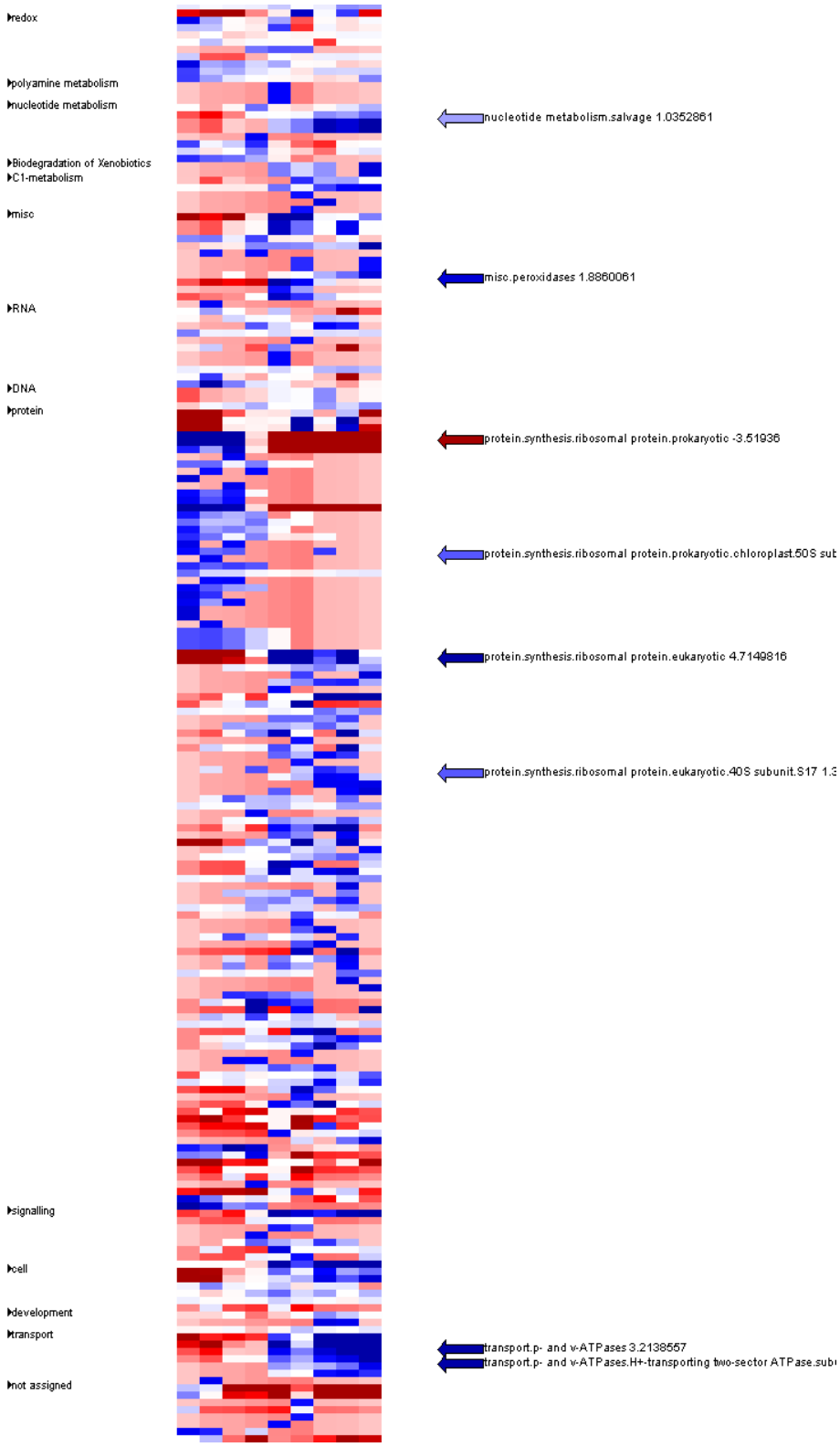

Figure 4.1. Hierarchical clustering of 528 proteins groups found in the nine fractions of *Arabidopsis thaliana* (page 39 and 40). The blue colour (from 2.1) represents the localization of the specific protein in the cell. The red colour (from -2.1) represents the non location or the lack of the specific protein in the cell. The white colour (0) represents the center of blue and red. The first lines of each section (PS, major CHO metabolism,….) represent a summary of all proteins in the nine fractions. For clustering the normalized spectral counts (PSM) of the nine fractions were used.

5. Outlook

So far, the NAF was used to calculate the percentage of the metabolite values in subcellular compartments of the cell. To determine the distribution of the metabolites in the compartment the activity of marker enzymes is used. The fact that this method allows an enzyme activity is an important indication for performing a large scale unbiased proteome experiment. The investigation presented here shows a possible establishment of a technique that allows the combined measurement of the metabolome and the proteome of leaves tissue under subcellular conditions. The establishment of a link from non- aqueous fractionation to proteomics allows a combined analysis of proteomics and metabolomics on a subcellular level and opens the door for new research questions:

- An analysis of the metabolome and proteome under the influence of various stress conditions and under subcellular conditions.
- The analyses of mutants for the better understanding of the distribution of the proteins and the metabolites in the different compartments of the cell.
- To link the combined non- aqueous fractionation measurement of the metabolome and the proteome to other research fields.

Targeted proteomics could be a very powerful technique for NAF. This could allow the precise determination of specific proteins such as the marker enzymes for the compartmentation analysis of the metabolites. The mass Western approach was developed for absolute quantification of different isoforms of proteins using the selective reaction monitoring (SRM) mode (Lehmann et al. 2008). With the powerful technique of SRM it is not only possible to quantify analytes with a known fragmentation pattern but also to detect them in a complex background (Picotti et al. 2012; Lange et al. 2008). In SRM a precursor ion and one of its fragments with the mass of the target peptide are selected by two mass filters of a triple quadrupole. Between the two quadrupoles a second quadrupole serves as collision cell. The transition of precursor / fragment ion pairs of the target peptides in combination with the retention time actually defines the assay. For absolute quantification the relative intensity of heavy isotope- labeled internal standard peptides can be compared with the analyte signals in a complex mixture. In this approach the targeted peptides are relatively quantified with heavy labeled peptides. For each subcellular compartment different standard peptides were designed *in silico* and synthesized by Thermo fisher "HeavyPeptide Custom Synthese Service".

Table 5.1. The heavy isotope- labeled internal standard peptides. For each compartment a standard peptide was designed and synthesized. The position of the labels (13C6;15N4) are shown in blue. In the case of Medtr_VaPe1 and Medtr_Cyt1 two sequences were concatenated. Each sequence was linked to an equalizer peptide.

name	target protein	location	labeled sequence	equalizer peptide
Medtr_Chl1	plastocyanine	chloroplast-lumen	NNAGFPHNVIFDEDEIPSGVDAA**K**	LVNE**L**TEFA**K**
Medtr_VaPe1	catalase	peroxisome	WVDALSDP**R**TWPEDIIPLQPVG**R**	LVNE**L**TEF**A**K
Medtr_VaPe2	v-type ATPase	vacuole	VGTLDSLLSLSDDLT**K**	L**V**NELTEF**A**K
Medtr_Cyt1	sucrose synthase	cytosol	VHSLKE**R**ALESEMLSE**R**	L**V**NE**L**TEFAK
Medtr_Mito2	aconitate hydratase	mitochondrion	GDEVVTIENLANVQP**R**	LVNETEFA**K**

Bibliography

Arabidopsis Genome Initiative. (2000) Analysis of the genome sequence of the flowering plant Arabidopsis thaliana. **408**, 796-815

Auria JC, Gershenzon J. The secondary metabolism of Arabidopsis thaliana: growing like a weed (2005) Current Opinion in Plant Biology **3,** 308-16

Bauwe, H., Hagemann, M., Kern, R. and Timm, S.(2012) Photorespiration has a dual origin and manifold links to centralmetabolism. Current Opinion in Plant Biology **15**, 269-275

Benkeblia, N., Shinano, T. and Osaki, M. (2007) Metabolite profiling and assessment of metabolome compartmentation of soybean leaves using non-aqueous fractionation and GC-MS analysis. Metabolomics **3**, 297-305

Bradford, M, (1976) A rapid and sensitive method for the quantitation of microgram quantities of protein utilizing the principle of protein-dye binding. Analytical biochemistry **72**, 248-254.

Carpentier, C., Witters, E., Laukens, K., Deckers, P., Swennen, R., Panis, B.(2005) Preparation of protein extracts from recalcitrant plant tissues: an evaluation of different methods for two-dimensional gel electrophoresis analysis.Proteomics **10,** 2497-507.

Daher, Z., Recorbet, G., Valot, B., Robert, F., Balliau, T., Potin, S., Schoefs, B and Dumas-Gaudot E (2011) Proteomic analysis of Medicago truncatula root plastids Proteomics **11**, 2123-37

Dietz, J., Tavakoli, N., Kluge, C., Mimura, T., Sharma, S., Harris, C., Chardonnens, N. and Golldack, D. (2001) Significance of the V-type ATPase for the adaptation to stressful growth conditions and its regulation on the molecular and biochemical level Journal of Experimental Botany **52,** 1969-80

Duve,C., Pressman, B., Gianetto, R., Wattiaux, R. and Appelmans, F. (1955).Tissue fractionation studies. 6. Intracellular distribution patterns of enzymes in rat-liver tissue. Biochemical Journal **4**, 604-17.

Eng, J., McCormack, A. and Yates, J. (1994) An approach to correlate tandem mass spectral data of peptides with amino acid sequences in a protein database. Journal of the American Society for Mass Spectrometry **5**, 976-989.

Farré, E., Tiessen, A., Roessner, U., Geigenberger, P., Trethewey, R. and Willmitzer, L.(2001) Analysis of the compartmentation of glycolytic intermediates, nucleotides, sugars, organic acids, amino acids, and sugar alcohols in potato tubers using a nonaqueous fractionation method. Plant Physiology **2**, 685-700

Geigenberger,P., Tiessen, A. and Meurer, J. (2011) Use of Non-aqueous Fractionation and Metabolomics to Study Chloroplast Function in Arabidopsis. Methods in Molecular Biology **775**, 135-160.

Gerhardt, R and Heldt H (1984) Measurement of subcellular metabolite levels in leaves by fractionation of freeze-stopped material in nonaqueous media **3**, 542-7

Glinski, M. and Weckwerth, W.(2006) The Role of mass spectrometry in plant systems Biology. Mass Spectrometry Reviews **2**, 173-214.

Goulas, E., Schubert, M., Kieselbach, T., Kleczkowski, A., Gardeström, P., Schröder, W. and Hurry, V.(2006) The chloroplast lumen and stromal proteomes of Arabidopsis thaliana show differential sensitivity to short- and long-term exposure to low temperature. Plant Journal **5**, 720-34

Heilmann, I., Mekhedov, S., King, B., Browse, J. and Shanklin, J.(2004) Identification of the Arabidopsis palmitoyl-monogalactosyldiacylglycerol delta7-desaturase gene FAD5, and effects of plastidial retargeting of Arabidopsis desaturases on the fad5 mutant phenotype. Plant Physiology **4**, 4237-4245.

Herman, M., Li, X., Su, T., Larsen, P., Hsu, H. and Sze, H. (1994) Vacuolar-Type H+ -ATPases Are Associated with the Endoplasmic Reticulum and Provacuoles of Root Tip Cells. Plant Physiology **4**, 1313-1324

Hu, H., Boisson, A., Israelsson, M., Böhmer, M., Xue, S., Ries, A., Godoski, J., Kuhn, M., Schroeder., I.(2010) Carbonic anhydrases are upstream regulators of CO2-controlled stomatal movements in guard cells. Nature Cell Biologie **1,** 87-93

Ilarslan, H., Palmer, R., Imsande, J and Horner, H. (1997) Quantitative determination of calcium oxalate and oxalate in developing seeds of soybean (Leguminosae). American Journal of Botany **8,** 1042

Ishihama Y, Rappsilber J, Mann M.(2006) Modular stop and go extraction tips with stacked disks for parallel and multidimensional Peptide fractionation in proteomics. J Proteome Res **4**, 988-94

Kherraz, K., Kherraz, K. and Kameli, A.(2011) Homology modeling of Ferredoxin-nitrite reductase from *Arabidopsis thaliana.* Bioinformation **3**, 115-119

Klie, S.,Krueger, S.,Krall. L.,Giavalisco,P., Flügge,U., Willmitzer,L. and Steinhauser, D.(2011) Analysis of the compartmentalized metabolome – a validation of the non-aqueous fractionation technique. Frontiers in plant science **2**, 55

Kluge, C., Lahr, J., Hanitzsch, M., Bolte, S., Golldack, D. and Dietz, K.(2003) New Insight Into the Structure and Regulation of the Plant Vacuolar H+-ATPase. Journal of Bioenergetics and Biomembranes **4**, 377-388

Knaupp, M., Mishra, BM., Nedbal, L. and Heyer, A.(2011) Evidence for a role of raffinose in stabilizing photosystem II during freeze-thaw cycles. Planta **234**, 477-486.

Krueger, S., Giavalisco, P., Krall, L., Steinhauser, C., Büssis, D., Usadel, B., Flügge, I., Fernie, R., Willmitzer, L., Steinhauser, D. (2011) A topological map of the compartmentalized Arabidopsis thaliana leaf metabolome. PLoS One **15**, 332-349.

Lange, V., Picotti, P., Domon, B. and Aebersold R. (2008) Selected reaction monitoring for quantitative proteomics: a tutorial Molecular Systems Biology **4** 222.

Lee, Y ., Tan, H. and Chung, M. (2010). Subcellular fractionation methods and strategies for proteomics. Proteomics **22**, 3935–3956.

Lehmann, S., Funck, D., Szabados, L. and Rentsch D. (2010) Proline metabolism and transport in plant development. Amino Acids **4**, 949 - 962.

Lehmann, U., Wienkoop, S., Tschoep, H. and Weckwerth, W.(2008) If the antibody fails- a mass western approach. Plant journal **6**, 1039-1046.

Matsuoka. K., Higuchi, T., Maeshima, M. and Nakamura, K. (1997) A Vacuolar-Type H+-ATPase in a Nonvacuolar Organelle Is Required for the Sorting of Soluble Vacuolar Protein Precursors in Tobacco Cells. Plant Cell **4**, 533-546.

Mereschkowsky, C. (1905) Über Natur und Ursprung der Chromatophoren im Pflanzenreiche. Biol Centralbl 25 593–604.

Mochizuki, N., Tanaka, R., Grimm, B., Masuda, T., Moulin, M., Smith, A., Tanaka, A. and Terry, M. (2010)The cell biology of tetrapyrroles: a life and death struggle. Trends in plant science **15**, 488-498.

Nadella,D., Marla,S. and Kumar, A.(2012) Metabolomics in agriculture. OMICS. **4** 149-59.

Young, N., Debellé, F., Oldroyd, G., Geurts., R. et al., (2011) The Medicago genome provides insight into the evolution of rhizobial symbioses. Nature **480**,520–524

Obata, T. and Fernie, R.(2012) The use of metabolomics to dissect plant responses to abiotic stresse Cellular and Molecular Life Sciences. **19** 3225-43**.**

Oikawa, A., Matsuda, F., Kikuyama, M., Mimura, T. and Saito. K.(2011) Metabolomics of a single vacuole reveals metabolic dynamism in an alga *Chara australis*. Plant Physiology **2**, 544-551.

Padmanaban, S., Lin, X., Perera, I., Kawamura, Y and Sze H. (2004) Differential expression of vacuolar H+-ATPase subunit c genes in tissues active in membrane trafficking and their roles in plant growth as revealed by RNAi. Plant Physiology **4**, 1514-26.

Peck, S. (2005) Update on Proteomics in Arabidopsis. Where Do We Go From Here? Plant Physiology **2**, 591–599.

Picotti, P. and Aebersold, R. (2012) Selected reaction monitoring-based proteomics: workflows, potential, pitfalls and future directions. Nature Methods **6,** 555-66

Rees A (*1987*) Compartmentation of plant metabolism.The Biochemistry of Plants. **12,** 87–115

Riens, B., Lohaus, G., Heineke, D. and Heldt, W. (1991) Amino Acid and sucrose content determined in the cytosolic, chloroplastic, and vacuolar compartments and in the Phloem sap of spinach leaves. Plant Physiology, **1** 227-33.

Saghatelian, A. and Cravatt, B. (2005) Global strategies to integrate the proteome and metabolome. Current Opinion in Chemical Biology **1**, 62-68.

Saito, K and Matsuda, F.(2010) Metabolomics for functional genomics, systems biology, and biotechnology. Annual Reviews Plant Biology **61**, 544-551

Shevchenko A, Tomas H, Havlis J, Olsen V, Mann M. (2006) In-gel digestion for mass spectrometric characterization of proteins and proteomes. Nature protocol **6**, 2856-60.

Siegenthaler, A. and Depéry, F. (1976) Influence of unsaturated fatty acids in chloroplasts. Shift of the pH optimum of electron flow and relations to delta pH, thylakoid internal pH and proton uptake. European Journal of Biochemistry **2**, 572-580

Staudinger C, Mehmeti V, Turetschek R, Lyon D, Egelhofer V, Wienkoop S. (2012) Possible role of nutritional priming for early salt and drought stress responses in Medicago truncatula. Frontiers in Plant Proteomics **3**, 285.

Stitt M, Lilley M, Gerhardt R, Heldt W. (1989) Metabolite levels in specific cells and subcellular compartments of plant leaves. Methods in Enzymology. 174 518–550

Talla, S., Riazunnisa, K., Padmavathi, L., Sunil, B., Rajsheel, P. and Raghavendra, A. (2011) Ascorbic acid is a key participant during the interactions between chloroplasts and mitochondria to optimize photosynthesis and protect against photoinhibition. Journal of Biosciences **1**, 163-173

Tiessen, A., Nerlich, A., Faix, B., Hümmer, C., Fox, S., Trafford, K., Weber, H., Weschke, W and Geigenberger, P. (2012) Subcellular analysis of starch metabolism in developing barley seeds using a non-aqueous fractionation method. **63**, 2071-87

Usadel, B., Nagel, A., Thimm, O., Redestig, H., Blaesing, OE., Palacios-Rojas, N., Selbig, J., Hannemann, J., Piques, C., Steinhauser, D., Scheible, R., Gibon, Y., Morcuende, R., Weicht, D., Meyer, S. and Stitt, M.(2005) Extension of the visualization tool MapMan to allow statistical analysis of arrays, display of corresponding genes, and comparison with known responses Plant Physiology, **3** 1195-204.

Usadel, B., Nagel, A., Steinhauser, D., Gibon, Y., Bläsing, E., Redestig, H., Sreenivasulu, N., Krall, L., Hannah, A., Poree, F., Fernie, R. and Stitt, M. (2006) PageMan: an interactive ontology tool to generate, display, and annotate overview graphs for profiling experiments. BMC Bioinformatics **7,** 535

Villarreal, F., Martín, V., Colaneri, A., González, N., Perales, M., Martín, M., Lombardo, C., Braun, P., Bartoli, C. and Zabaleta, E. (2009) Ectopic expression of mitochondrial gamma carbonic anhydrase 2 causes male sterility by anther indehiscence Plant Mololecular Biology **4,** 471-85

Washburn, P., Wolters, D. and Yates, R.(2001) Large-scale analysis of the yeast proteome by multidimensional protein identification technology **3**, 242-7

Weckwerth, W., Wenzel, K., Fiehn, O. (2004) Process for the integrated extraction, identification and quantification of metabolites, proteins and RNA to reveal their co-regulation in biochemical networks. Proteomics **4**, 78-83.

Wienkoop, S., Weiss, J., May, P., Kempa, S., Irgang, S., Recuenco, L., Pietzke, M., Schwemmer, T., Rupprecht, J., Egelhofer, V. and Weckwerth, W. (2010) Targeted proteomics for Chlamydomonas reinhardtii combined with rapid subcellular protein fractionation, metabolomics and metabolic flux analyses. Molecular BioSystems **6**, 1018-1031

Wienkoop, S., Staudinger, C., Hoehenwarter, W., Weckwerth, W. and Egelhofer, V.(2012) ProMEX - a mass spectral reference database for plant proteomics frontiers in plant science **3** 125.

Wienkoop, S., Glinski, M., Tanaka, N., Tolstikov, V., Fiehn, O. and Weckwerth, W.(2004) Linking protein fractionation with multidimensional monolithic reversed-phase peptide chromatography/ mass spectrometry enhances protein identification from complex mixtures even in the presence of abundant proteins. Rapid Communications in Mass Spectrometry **6** 643-50.

6. Acknowledgements

The last words of my thesis are dedicated to all the great people who accompanied and supported me during my Diploma thesis and my undergraduate studies.

Mein allergrößtes Dankeschön gilt natürlich zunächst **Wolfram Weckwerth** und **Stefanie Wienkoop**. Ich danke Ihnen für meine Diplomstelle und außerdem für das große Vergnügen, das ich während meiner Arbeit hatte. Liebe Stefanie, vielen lieben Dank, dass ich bei Dir so viele verschiedene Methoden ausprobieren durfte und dadurch gelernt habe selbstständig Probleme zu lösen zu können.

Ein herzliches Dankschön geht an **meine Eltern, meine Schwester Minzi** und an meine **Oma**. Danke für die Unterstützung und das starke Interesse an meinem Werdegang und die Motivation in die Naturwissenschaft zu gehen. Ich habe es immer genossen wie Franz am Abend am Tisch gesagt hat: „Was gib es Neues in der Wissenschaft“. Meiner Mutter will ich besonders danken für ihre Geduld mit mir und vor allem für ihre sanfte Art. Auch **Ulrike Albrecht** möchte ich erwähnen, danke für das Wecken meines Interesses an der Chemie.

A big thanks to all people at Mosys that have accompanied me during my thesis. First of all many thanks to **Thomas Nägele** for bringing the powerful non- aqueous fractionation technique to the lab and for the quick establishment of this technique. For solving problems in the lab I will thank **Christiana, Vlora, David, Maria Angeles, Reinhard, Till, Luis, Lena, Mette, Ella**.

Affirmation

I declare that my Diploma Thesis was written on my own having used only the listed resources and tools.

Erklärung

Die vorgelegte Arbeit wurde von mir selbständig angefertigt und nur die angegebenen Hilfsmittel benutzt. Alle Stellen, die dem Wortlaut oder den Sinne nach anderen Werken entnommen wurden, sind durch Angabe der Quelle kenntlich gemacht wurden

Wien, am

Benedict Dirnberger

A. Attachment

A.1. Summary

The establishment for an integrative approach for metabolomics and proteomics studies on subcellular level will lead to a more differentiated and comprehensive analysis of the complex plant cell metabolism. Special techniques that enable combined metabolomic and proteomic research on subcellular level are a bottle neck in the field of subcellular research. The non- aqueous fractionation (NAF) was developed as a powerful technique that allows the separation of plant material, especially leaves, into a series of fractions (Stitt et al. 1989). Non- aqueous fractionation is currently the only method that allows calculating the distribution of metabolites in plant tissues (Geigenberger et al. 2011). The determination of the distribution of subcellular metabolites among chloroplast, cytosol/mitochondrion and vacuole is done via marker enzyme activities. These marker enzymes are selective for each compartment. Markers that are shared between compartments could lead to errors in the calculation. Although established for metabolomics, NAF has not been used for proteomic analysis, so far. An adaptation of this technique for proteomic shotgun mass spectrometry based studies will enable the investigation of the subcellular distribution of the proteome and the discovery of novel marker enzymes which are important to determine the quantitative distribution of metabolites across the cellular compartments.

This thesis gives first insights into a combined technique using NAF to investigate the metabolome and the proteome on a subcellular level. The main focus of this study was the prove of concept for applicability of NAF to proteomics. Subcellular fractions of a NAF gradient were analyzed for *Arabidopsis thaliana* and *Medicago truncatula* leave tissue using mass spectrometry. Besides these measurements it could be shown that it is possible not only to identify the well known marker enzymes but to also identify new and robust marker enzymes and improve the quantitative determination of the distribution of the metabolites with these new marker enzymes. For analyzing the metabolite concentration in the nine fractions gas chromatography mass spectrometry was used. With the help of the marker enzymes it is possible to define the distribution of the metabolites in the different compartments. To determine efficiency of the NAF, this fractionation has been compared with other well known “percoll gradient” extraction protocols.

The progress of the NAF to a proteomic level opens new doors for further research questions. One of them addresses the changes in the metabolites and proteins under different environmental conditions such as under drought or different salt conditions. The integrative NAF approach will also allow for absolute quantification of marker enzymes using targeted proteomics such as mass western (Lehmann et al. 2008). The absolute quantification of marker enzymes would enable to determine the distribution of the proteins and metabolites in the different compartments on absolute concentration level. My thesis will also show an initial approach to set up specific mass western for subcellular fractionation.

A.2. Zusammenfassung

Die Etablierung von Techniken, die es erlauben auf subzellularer Ebene das Metabolom gemeinsam mit dem Proteom untersuchen zu können, führen zu einem besseren Verständnis des komplexen Zellmetabolismus der Pflanze. Spezielle Methoden, die es vor allem möglich machen, kombinierte Metabolomik und Proteomik auf subzellularer Ebene betreiben zu können, sind ein Engpaß auf dem Gebiet der subzellulären Forschung. Die "Nicht-wässrige Fraktionierung" wurde als bahnbrechende Technologie entwickelt, die es erlaubt, zelluläre Pflanzengewebe, insbesondere Blätter, in verschiedene Fraktionen zu trennen (Stitt et al. 1989). Sie ist derzeit die einzige Methode, um die Verteilung der Metaboliten in Pflanzengewebe berechnen zu können (Geigenberger et al. 2011). Sie erlaubt die quantitative Bestimmung der Verteilung der Metaboliten in den Chloroplasten beziehungsweise in Zytosol/Mitochondrien und in den Vakuolen mit Hilfe von Messungen der Markerenzymaktivitäten. Diese Markerenzyme sind spezifisch für das jeweilige Zellkompartiment. Marker, welche in verschiedenen Kompartimenten aktiv sind, führen zu Fehlern in der Berechnung. Obgleich etabliert für Metabolomik ist die „Nicht- wässrige Fraktionierung" bislang nicht für Analysen in der Proteomik verwendet worden. Eine weiterführende Entwicklung dieser Methode für Proteomik auf Basis einer „shotgun" massenspektroskopischen Analyse ermöglicht nicht nur die Erforschung der subzellulären Lokalisation von Proteinen, sondern zugleich auch das Auffinden neuer Markerenzyme, die für die quantitative Bestimmung der Verteilung der Metaboliten wichtig sind.

Die vorliegende Arbeit bietet erste Einblicke in eine kombinierte Technik der "Nicht-wässrigen Fraktionierung" zur Untersuchung der Metabolome und Proteome auf subzellulärer Ebene. Ein Hauptaugenmerk liegt auf der Etablierung der "Nicht-wässrigen Fraktionierung" hin zur Untersuchung des Proteoms eines Pflanzengewebes. Subzelluläre Fraktionierungen eines gradienten wurden für Pflanzengewebe von *Arabidopsis thaliana* und *Medicago truncatula* mittels Massenspektroskopie analysiert. Außerdem wurde gezeigt, dass es mit dieser Technik möglich ist, nach verschieden geeigneten Markerenzymen suchen zu können und mit diesen dann die quantitative Bestimmung der Verteilung der Metabolite durchzuführen. Zur Bestimmung der verschiedenen Metabolitkonzentrationen in den neun Fraktionen des gleichen Gradienten wurde eine gaschromatograph- massenspektrometrische Analyse herangezogen. Mit Hilfe der Markerenzyme ist es möglich, die quantitative Verteilung der Metabolite in den Zellkompartimenten bestimmen zu können. Um die Effektivität der "Nicht-wässrigen Fraktionierung" zu bestimmen wurde diese Fraktionierung verglichen mit anderen bekannten „Percoll gradient" Extraktions Protokollen.

Durch Weiterentwicklung dieses Verfahrens können neue Türen für wesentliche zusätzliche Fragestellungen geöffnet werden. Eine davon wäre zum Beispiel die Untersuchung der Veränderung des Metaboloms beziehungsweise Proteoms auf subzellulärer Ebene nach geänderten Umweltbedingungen, zum Beispiel unter bestimmten Trockenbedingungen beziehungsweise veränderten Salzkonzentrationen. Der integrative Ansatz der "Nicht-wässrigen Fraktionierung" wird die absoulte Quantifizierung von Markerenzymen mittels „targeted proteomics" wie zum Beispiel Mass Western möglich machen (Lehmann et al. 2008). Die absolute Quantifizierung der Markerenzyme wird die Bestimmung der Verteilung der Proteine und Metabolite in den verschienen zellulären Kompartments auf Basis ihrer Konzentration ermöglichen. Meine Arbeit gibt einen kurzen Einblick in die Mass Western Technik für subzellulärer Fraktionierung.

Table A.1: 528 protein groups in *Arabidopsis thaliana*

Accession number	Protein description	PSM1	PSM2	PSM3	PSM4	PSM5	PSM6	PSM7	PSM8	PSM9
AT4G03520.2	Thioredoxin superfamily protein		7		6					
ATCG00480.1	ATP synthase subunit beta	282	327	290	286	180	155	110	99	90
AT4G02520.1	glutathione S-transferase PHI 2	18	23	25	42	40	52	24	33	39
AT5G15970.1	stress-responsive protein (KIN2)	10	9	12	9	14	11	15	17	
ATCG00470.1	ATP synthase epsilon chain	18	22	20	19	11	9	7	7	4
AT2G23120.1	Late embryogenesis abundant protein						7			
AT2G39730.1	rubisco activase	208	227	221	188	142	123	66	47	39
AT1G06680.2	photosystem II subunit P-1	67	58	53	52	30	30	23	18	13
AT2G27710.1	60S acidic ribosomal protein family		7	7	9	7	10	7	8	5
AT1G13440.1	glyceraldehyde-3-phosphate dehydrogenase	13	30	46	56	49	67	43	45	51
AT3G04120.1	glyceraldehyde-3-phosphate dehydrogenase	13	30	46	56	49	69	44	48	51
AT5G66570.1	PS II oxygen-evolving complex 1	138	128	93	98	76	65	27	47	33
ATCG00490.1	ribulose-bisphosphate carboxylases	447	626	726	614	384	416	166	215	200
AT5G38410.1	Ribulose bisphosphate carboxylase	206	223	288	212	122	117	32	54	39
AT1G67090.1	ribulose bisphosphate carboxylase	219	227	287	214	121	134	42	65	46
AT1G32060.1	phosphoribulokinase	54	63	54	57	31	27	17	5	9
AT3G50820.1	photosystem II subunit O-2	117	108	95	98	73	64	25	37	30
AT5G09660.2	peroxisomal NAD-malate dehydrogenase 2	7	23	33	26	20	19	16	13	13
AT1G02930.1	glutathione S-transferase 6		4	7	12	9	21	7	5	18
AT4G09650.1	ATP synthase delta-subunit gene	29	38	35	29	18	13	10	4	7
AT4G02770.1	photosystem I subunit D-1	44	47	39	41	32	23	13	7	19
AT3G12780.1	phosphoglycerate kinase 1	78	98	91	84	59	54	35	34	29
AT3G14415.1	Aldolase-type TIM barrel family protein	11	18	31	34	28	36	24	18	24
AT3G14420.1	Aldolase-type TIM barrel family protein	9	17	32	37	28	33	24	17	23
AT3G55440.1	triosephosphate isomerase	4	16	16	21	28	30	14	12	18
AT1G01100.1	60S acidic ribosomal protein family				4		5	3		
AT5G20720.1	chaperonin 20	34	33	28	30	18	15	11	7	5
AT2G27720.1	60S acidic ribosomal protein family			4	6	7	8	6	7	5
ATCG00120.1	ATP synthase subunit alpha	120	165	159	154	113	87	67	66	54
AT1G13930.1	Involved in response to salt stress	4	9	11	13	14	13	6	13	9
AT5G08670.1	ATP synthase alpha/beta family protein	51	50	54	65	60	62	56	42	42
AT5G40370.1	Glutaredoxin family protein				2	5	5	5	5	3
AT3G60750.2	Transketolase	69	85	92	61	50	48	31	31	26
AT5G38430.1	Ribulose bisphosphate carboxylase	194	201	269	188	113	114	26	54	39
AT1G53240.1	Lactate/malate dehydrogenase family protein	24	28	29	26	23	22	18	15	15
AT4G09000.1	general regulatory factor 1	2	9	13	15	34	39	26	32	26
AT4G37930.1	serine transhydroxymethyltransferase 1	35	40	41	50	51	45	30	36	28
AT4G38970.1	fructose-bisphosphate aldolase 2	100	114	106	99	68	63	49	40	29
AT3G26650.1	glyceraldehyde 3-phosphate dehydrogenase A	91	108	104	109	96	79	69	44	43
AT2G47730.1	glutathione S-transferase phi 8	8	7	13	16	21	21	12	11	11
AT2G30860.1	glutathione S-transferase PHI 9	5	19	22	23	17	28	17	19	17
AT2G28000.1	chaperonin-60alpha	64	68	58	54	49	42	26	21	13

AT5G35630.1	glutamine synthetase 2	56	59	59	51	29	33	17	12	6
AT3G20390.1	endoribonuclease L-PSP family protein	11	7	7	7	8	4	5	4	3
AT1G02920.1	glutathione S-transferase 7		4	5	8	12	13	7	3	16
AT1G12900.3	glyceraldehyde 3-phosphate dehydrogenase A	57	77	69	66	49	46	29	22	35
AT2G20260.1	photosystem I subunit E-2	12	14	8	10	8	6		6	6
AT3G27850.1	ribosomal protein L12-C	28	23	19	18	13	10	7	8	5
AT3G17390.1	S-adenosylmethionine synthetase		7	18	15	10	30	11		13
AT1G04410.1	Lactate/malate dehydrogenase family	7	13	20	19	27	28	22	17	28
AT3G52930.1	Aldolase superfamily protein	5	14	24	23	26	27	8	24	21
AT2G30870.1	glutathione S-transferase PHI 10		4	4	9	6	11	3	6	7
AT5G66190.1	ferredoxin-NADP(+)-oxidoreductase 1	35	46	35	30	19	14	7	5	8
AT4G21280.1	photosystem II subunit QA	65	61	55	55	46	33	20	20	15
AT1G68010.1	hydroxypyruvate reductase	3	8	22	16	15	20	16	8	9
AT3G47070.1	unknown protein	15	16	14	13	12	7	9	3	5
AT1G76030.1	ATPase, V1 complex, subunit B protein			4	10	20	24	17	19	20
AT4G04640.1	ATPase, F1 complex, gamma subunit protein	38	42	37	33	13	14	6	3	8
AT3G52960.1	Thioredoxin superfamily protein	18	17	14	16	9	5			
AT1G42970.1	glyceraldehyde-3-phosphate dehydrogenase B	62	94	84	68	50	46	30	24	35
AT5G17920.1	Cobalamin-independent synthase family protein	16	42	64	74	78	97	83	60	57
AT1G56190.2	Phosphoglycerate kinase family protein	37	49	45	44	28	27	21	16	14
AT4G02530.1	chloroplast thylakoid lumen protein	15	21	14	13	11	4	5	3	
AT4G20360.1	RAB GTPase homolog E1B	77	76	64	66	40	37	24	20	16
AT3G11630.1	Thioredoxin superfamily protein	51	50	45	44	36	26	22	19	12
AT4G38510.1	ATPase, V1 complex, subunit B protein			4	9	15	20	14	14	16
AT2G37220.1	RNA-binding (RRM/RBD/RNP motifs)	34	36	20	24	13	7	8	5	5
AT5G14740.2	carbonic anhydrase 2	56	76	68	70	72	75	53	58	52
AT4G05180.1	photosystem II subunit Q-2	56	50	44	45	33	24	20	20	14
AT3G14210.1	epithiospecifier modifier 1		12	36	49	50	61	51	74	75
AT5G02500.1	heat shock cognate protein 70-1	10	24	33	43	27	46	29	38	29
AT3G04790.1	Ribose 5-phosphate isomerase, type A	19	20	17	19	9	6	4		
AT1G20020.2	ferredoxin-NADP(+)-oxidoreductase 2	33	37	27	26	12	9	4		
AT3G16640.1	translationally controlled tumor protein		4	6	11	13	14	13	5	9
AT1G09340.1	chloroplast RNA binding	16	23	24	19	7	10	7	6	5
AT2G43030.1	Ribosomal protein L3 family protein	19	13	11	10	7				
AT2G21330.1	fructose-bisphosphate aldolase 1	80	97	92	81	53	48	33	33	31
ATCG00540.1	photosynthetic electron transfer A	23	26	11	13	4	5			5
AT3G47470.1	light-harvesting chlorophyll-protein complex I	17	20	20	14	8	4		5	5
AT3G55800.1	sedoheptulose-bisphosphatase	65	66	49	51	34	32	15	9	16
AT1G55490.1	chaperonin 60 beta	37	43	36	33	23	20	12	12	11
AT1G23310.1	glutamate:glyoxylate aminotransferase	13	18	27	25	24	22	17	16	21
AT5G26000.2	thioglucoside glucohydrolase 1	25	30	39	40	42	30	21	19	9
AT4G26530.1	Aldolase superfamily protein	6	16	15	16	22	24	13	14	13
AT3G57260.1	beta-1,3-glucanase 2			7	12	17	15	10	10	7
AT5G38480.2	general regulatory factor 3	2	8	12	11	21	25	19	22	12
AT1G07890.6	ascorbate peroxidase 1		8	10	10	11	12	8	5	11
AT1G03680.1	thioredoxin M-type 1	21	23	17	17	13	10	3	3	4

AT1G54780.1	thylakoid lumen 18.3 kDa protein	9	12	7	7	2				
AT1G78300.1	general regulatory factor 2	2	8	12	12	25	28	21	27	18
AT3G01500.3	carbonic anhydrase 1	83	95	86	83	85	82	58	61	56
AT5G19510.1	Translation elongation factor EF1B		3	5	7	9	5	9	5	7
AT2G36460.1	Aldolase superfamily protein	5	9	10	13	15	22	6	13	10
AT4G39260.3	cold, circadian rhythm, and RNA binding 1	3	8	9	10	11	10	9	10	6
AT5G54770.1	thiazole biosynthetic enzyme, chloroplast	5	10	10	7	3		3		
AT1G20620.5	catalase 3	4	8	22	20	18	33	21	24	25
AT5G06290.1	2-cysteine peroxiredoxin B	41	37	32	31	26	19	16	14	8
AT4G39200.2	Ribosomal protein S25 family protein					3			3	5
AT1G11860.1	Glycine cleavage T-protein family	14	21	20	28	12	20	11	13	11
AT2G34420.1	photosystem II light harvesting complex	38	43	34	36	26	28	13	16	8
AT2G36530.1	Enolase		9	13	12	16	24	18	18	22
AT1G29910.1	chlorophyll A/B binding protein 3	41	48	38	42	26	28	13	16	8
AT4G20260.1	plasma-membrane associated cation-binding					5	9	4	4	5
AT4G10340.1	light harvesting complex of photosystem II 5	14	25	22	19	11	12	7	4	6
AT1G23410.1	Ribosomal protein S27a / Ubiquitin family	5	7	7	13	13	14	4	11	8
AT5G10450.2	G-box regulating factor 6	2	4	6	7	16	23	17	21	16
AT3G18780.1	actin 2		4	10	8	15	31	10	16	16
AT3G08740.1	elongation factor P (EF-P) family protein	8	2	3	4					
AT3G49010.4	breast basic conserved 1		7	6	7	7	10	10	11	
AT2G05220.1	Ribosomal S17 family protein		3		4		4	4	3	
AT4G03280.2	photosynthetic electron transfer C	17	22	19	23	14	9	8	4	5
AT1G09310.1	Protein of unknown function, DUF538					5	10	5	6	6
AT1G26630.1	Eukaryotic translation initiation factor 5A-1				3	8	9	7	5	10
AT1G61520.2	photosystem I light harvesting complex gene 3	19	24	24	22	11	12	8	7	4
AT2G37190.1	Ribosomal protein L11 family protein	3	4	7	10	8	12		8	5
AT1G10630.1	ADP-ribosylation factor A1F						7	3		
AT2G21170.1	triosephosphate isomerase	20	19	17	20	10	8	3		3
AT2G16600.2	rotamase CYP 3			2	7	8	7	7	3	3
AT2G24940.1	membrane-associated progesterone							2		
AT2G41840.1	Ribosomal protein S5 family protein			5	4	5	11	6	4	4
AT3G26060.1	Thioredoxin superfamily protein	16	14	10	9	7	4	3		
AT4G25050.1	acyl carrier protein 4	15	14	11	9	4	6			
AT3G61470.1	photosystem I light harvesting	7	11	9	8	3				
AT2G13360.1	alanine:glyoxylate aminotransferase	9	10	22	13	15	15	12	6	8
AT1G31812.1	acyl-CoA-binding protein 6				4	5			2	4
AT2G21660.1	cold, circadian rhythm, and rna binding 2	6	14	14	13	14	15	15	16	9
AT1G22780.1	Ribosomal protein S13/S18 family					4	8	10	9	2
AT4G28750.1	Photosystem I reaction centre subunit IV	17	15	14	13	9	7		6	5
AT1G48030.1	mitochondrial lipoamide dehydrogenase 1	3	6	6	8	7	9	7	4	
AT1G56070.1	Ribosomal protein S5/Elongation factor G	7	15	21	22	26	46	25	22	22
AT1G79040.1	photosystem II subunit R		11	10	11	5	5			
AT3G09200.2	Ribosomal protein L10 family protein	5	12	12	12	12	20	7	5	6
AT2G19740.1	Ribosomal protein L31e family protein			4	4	4	5			
AT3G09440.1	Heat shock protein 70 (Hsp 70)	7	11	16	18	19	29	25	28	23
AT4G13940.1	S-adenosyl-L-homocysteine hydrolase		4	13	16	18	31	17	22	20

AT1G23740.1	Oxidoreductase, zinc-binding dehydrogenase	9	12	6	11	3	4		2	
AT3G13920.3	eukaryotic translation initiation factor 4A1		3	7	11	8	13	8	9	11
AT4G32260.1	ATPase, F0 complex, subunit B/B', bacterial/chloroplast	15	17	13	10	8	6	6	5	
AT1G78900.1	vacuolar ATP synthase subunit A			4	4	13	17	10	24	13
AT2G18020.1	Ribosomal protein L2 family	2	4	9	12	7	15	6	10	8
AT5G42980.1	thioredoxin 3		2	3	4	6	4	4	4	4
AT4G09320.1	Nucleoside diphosphate kinase family protein		4	7	5	6	6		7	8
AT3G10090.1	Nucleic acid-binding, OB-fold-like protein				3					
AT2G28190.1	copper/zinc superoxide dismutase 2	7	8	9	5					
AT2G37660.1	NAD(P)-binding Rossmann-fold superfamily	24	23	22	22	13	11	5		4
ATCG00780.1	ribosomal protein L14		5	3						
AT5G07090.2	Ribosomal protein S4 (RPS4A) family					5	11	7	7	3
AT3G03780.1	methionine synthase 2	4	17	30	36	36	52	36	24	30
AT1G03600.1	photosystem II family protein	8	10	10	6	5		4		
AT3G02520.1	general regulatory factor 7	2	8	12	11	19	24	16	19	11
AT1G16880.1	uridylyltransferase-related	7	5	4	11	3	2			
AT2G43750.1	O-acetylserine (thiol) lyase B	11	8	7	9	7	2			
AT4G24770.1	31-kDa RNA binding protein	38	32	30	24	20	14	8	3	2
AT3G52150.1	RNA-binding (RRM/RBD/RNP motifs) family	10	11	9	9	6				
AT3G45140.1	lipoxygenase 2	26	27	32	29	15	12	7		
AT5G20290.1	Ribosomal protein S8e family protein	4	6	9	8	10	11	13	10	9
AT2G35370.1	glycine decarboxylase complex H	15	18	19	20	14	13			
AT5G49910.1	chloroplast heat shock protein 70-2	25	29	21	22	7	11	9	2	3
AT3G63140.1	chloroplast stem-loop binding protein	19	24	20	16	6	7	3		
AT5G15200.2	Ribosomal protein S4					5	9	3	4	
AT5G14910.1	Heavy metal transport/detoxification superfamily	9	10	5	3	6				
AT1G15820.1	light harvesting complex photosystem II subunit 6	7	10	6	6	6	6	4	4	3
AT3G23810.1	S-adenosyl-l-homocysteine (SAH) hydrolase 2		2	8	7	10	23	18	15	13
AT5G15960.1	stress-responsive protein (KIN1) /									4
AT5G53490.2	Tetratricopeptide repeat (TPR)	6	7	3	4					
AT4G14960.1	Tubulin/FtsZ family protein			6	5	8	17	11	12	9
AT1G04270.2	cytosolic ribosomal protein S15					5	5	6	4	
AT1G32470.1	Single hybrid motif superfamily protein	16	18	19	20	13	10			
AT5G61410.1	D-ribulose-5-phosphate-3-epimerase	7	10	9	10	5				
AT3G63190.1	ribosome recycling factor, chloroplast precursor	9	11	9	7	4				
AT3G49120.1	peroxidase CB			3		5	8	7	9	25
AT5G36790.1	Haloacid dehalogenase-like hydrolase (HAD)	15	11	9	9	7	4	3		
AT4G15802.1	heat shock factor binding protein				2					
AT1G02500.1	S-adenosylmethionine synthetase 1		4	10	9	4	12	7		8
AT3G03250.1	UDP-GLUCOSE PYROPHOSPHORYLASE 1				3	2	13	4	3	
AT4G35090.1	catalase 2	10	16	20	19	14	16	6	6	11
AT5G42020.1	Heat shock protein 70 (Hsp 70) family protein		5	6	13	15	29	19	16	12
AT5G28540.1	heat shock protein 70 (Hsp 70) family protein		5	6	15	15	30	20	17	13
AT4G18480.1	P-loop containing nucleoside triphosphate	13	15	9	8	6	2			
AT1G35720.1	annexin 1			2	4	10	14	8	7	7
AT1G02780.1	Ribosomal protein L19e family protein						7	6		

AT2G36160.1	Ribosomal protein S11 family protein		3	3	3	4	3		4	
AT3G11510.1	Ribosomal protein S11 family protein		3		2	3	4		4	3
AT4G24280.1	chloroplast heat shock protein 70-1	23	23	17	19	7	8	9	2	3
AT5G44340.1	tubulin beta chain 4			5	3	6	18	13	12	5
AT1G43670.1	Inositol monophosphatase family protein	4	6	4	5	10	11	6	7	
AT4G11150.1	vacuolar ATP synthase subunit E1					6	7	4	5	10
AT1G14980.1	chaperonin 10				3	3	2			
AT1G79850.1	ribosomal protein S17	5	4	4	2					
AT1G19570.2	dehydroascorbate reductase			3	3	4	4		4	8
AT3G49910.1	Translation protein SH3-like family protein	3	2	4	4	4	5		5	4
AT3G54050.1	high cyclic electron flow 1	24	27	25	21	15	11			5
AT5G59880.1	actin depolymerizing factor 3						5	2		4
AT3G02560.1	Ribosomal protein S7e family protein		6	5	8	5	10			
AT2G24200.1	Cytosol aminopeptidase family protein				5	14	13	13	7	7
AT3G44310.1	nitrilase 1	5	10	12	17	25	25	26	21	13
AT1G43170.4	ribosomal protein 1			5	4	7	7	4		8
ATCG00830.1	ribosomal protein L2	14	12	10	13	8	8			
AT3G48730.1	glutamate-1-semialdehyde 2,1-aminomutase 2	8	12	8	6	2	3			
AT2G05070.1	photosystem II light harvesting complex gene 2.2	16	22	14	15	10	11	8	8	5
AT5G50920.1	CLPC homologue 1	21	29	28	26	11	14	5	5	
AT3G23400.1	Plastid-lipid associated protein PAP / fibrillin family protein	9	7	4	6	3				
AT1G07920.1	GTP binding Elongation factor Tu family protein	9	26	48	44	51	52	31	44	28
AT3G45030.1	Ribosomal protein S10p/S20e family protein							3	3	3
AT3G46030.1	Histone superfamily protein		4	5	6	4	5	5	3	4
AT1G31330.1	photosystem I subunit F	8	8	4	3	4	4	4	5	4
AT4G31700.2	ribosomal protein S6			2		3	4	6	6	5
AT1G22300.3	general regulatory factor 10		5	7	6	11	18	13	14	10
AT4G04020.1	fibrillin	7	6	5	4					
AT2G36880.1	methionine adenosyltransferase 3		4	11	6	6	13	6		9
AT1G48350.1	Ribosomal L18p/L5e family protein	4	2	3						
AT1G79550.1	phosphoglycerate kinase	8	10	8	11	14	13	13	12	12
AT3G05560.1	Ribosomal L22e protein family						5		3	
AT5G27770.1	Ribosomal L22e protein family						3		4	
AT5G58330.3	lactate/malate dehydrogenase family protein	7	5	4	4					
AT5G23120.1	photosystem II stability/assembly factor,	14	12	8	11	2	3			
AT1G66970.1	SHV3-like 2				9	24	29	18	9	
AT3G04840.1	Ribosomal protein S3Ae			3		6	6	5	7	
AT1G65960.2	glutamate decarboxylase 2						10	2	3	3
AT3G62030.3	rotamase CYP 4	24	17	14	22	8	6		5	
AT3G63490.1	Ribosomal protein L1p/L10e family	12	9	6	7		4			
AT3G53460.1	chloroplast RNA-binding protein 29	9	13	7	7	6	3	2		3
AT5G09650.1	pyrophosphorylase 6	12	12	8	7	3				
AT2G21530.1	SMAD/FHA domain-containing protein	5	3		2					
ATCG00580.1	photosystem II reaction center protein E		4							
AT4G39330.2	cinnamyl alcohol dehydrogenase 9						6	5	2	2
AT3G12110.1	actin-11			4	3	8	19	6	8	16

AT1G53850.1	20S proteasome alpha subunit E1					3	4		2	
AT3G14290.1	20S proteasome alpha subunit E2					3	3		2	
AT3G46780.1	plastid transcriptionally active 16	13	13	6	4		2			
AT4G34870.1	rotamase cyclophilin 5					6	7	3		3
AT1G29670.1	GDSL-like Lipase/Acylhydrolase superfamily					5	8	3		
AT5G22580.1	Stress responsive A/B Barrel Domain		3	4	6	6	6	7	5	7
AT5G04140.1	glutamate synthase 1	18	30	39	24	22	16	6	5	
AT3G09630.2	Ribosomal protein L4/L1 family			6	5	5	15	9	5	
AT3G06050.1	peroxiredoxin IIF					3	4			
AT2G20270.1	Thioredoxin superfamily protein	2								
AT3G44890.1	ribosomal protein L9	5	4	3				3		
AT1G57720.1	Translation elongation factor EF1B, gamma chain					5	12	6	7	4
AT4G29350.1	profilin 2				6	5	7	7		
AT2G42540.3	cold-regulated 15a	4	4	3	3					
AT3G52880.1	monodehydroascorbate reductase 1			2		8	10	7	8	8
AT3G09820.1	adenosine kinase 1			4	4	8	11	10	8	8
AT2G42530.1	cold regulated 15b	5	4	2	2	4				
AT4G18100.1	Ribosomal protein L32e		3	3	6	4	6			
AT5G46430.1	Ribosomal protein L32e		2		4	3	4			
AT4G27090.1	Ribosomal protein L14						6			
AT1G07320.3	ribosomal protein L4	12	11	5	8	2	2	2		
AT2G44650.1	chloroplast chaperonin 10	9	6	5	6					
AT3G56340.1	Ribosomal protein S26e family protein		3	5	4	4	5		4	
ATCG00670.1	plastid-encoded CLP P	4	5	6	5					
AT4G16500.1	Cystatin/monellin superfamily protein					3				
AT3G47520.1	malate dehydrogenase	8	6	8	7					
AT5G03300.1	adenosine kinase 2					2	5	3	3	3
AT1G76100.1	plastocyanin 1		6	3	5		6			
AT2G38230.1	pyridoxine biosynthesis 1.1		6	8	8	5	7		7	3
AT1G69620.1	ribosomal protein L34				3		3			2
AT2G42590.2	general regulatory factor 9		3	3	4	9	11	8	12	6
AT3G25520.1	ribosomal protein L5		4	4	5	5	11	7	8	4
AT1G07660.2	Histone superfamily protein					2			2	
AT1G26880.1	Ribosomal protein L34e superfamily protein				3		3			3
AT3G04400.2	Ribosomal protein L14p/L23e family protein			2		3	2	2	5	
ATCG00790.1	ribosomal protein L16	5	3							
AT2G45470.1	FASCICLIN-like arabinogalactan protein 8					6	7			
AT5G63570.1	glutamate-1-semialdehyde-2,1-aminomutase	10	9	9	8		2			
AT3G12390.1	Nascent polypeptide-associated complex (NAC), alpha subunit family protein					4	3	4	2	2
AT1G18540.1	Ribosomal protein L6 family protein					4	5			4
AT1G15930.2	Ribosomal protein L7Ae/L30e/S12e/Gadd45 family			2	2	4	4		3	
AT1G62750.1	Translation elongation factor EFG/EF2 protein	17	24	20	14	9	12	5	2	
AT5G43940.1	GroES-like zinc-binding dehydrogenase family						7			2
AT5G02870.2	Ribosomal protein L4/L1 family		3	7	7	7	13	11	7	2
AT5G20630.1	germin 3					13	11	7		
AT1G23290.1	Ribosomal protein L18e/L15 superfamily protein				2	4	4	3		

AT5G19770.1	tubulin alpha-3			6	5	9	16	13	13	10
ATCG01060.1	iron-sulfur cluster binding;electron carriers		10	7	5					
AT5G40950.1	ribosomal protein large subunit 27	5								
AT2G07698.1	ATPase, F1 complex, alpha subunit protein	10	24	27	22	28	33	18	16	18
AT3G53870.1	Ribosomal protein S3 family protein						3			2
ATCG00130.1	ATPase, F0 complex, subunit B/B', bacterial/chloroplast	3	5		2					
AT2G38540.1	lipid transfer protein 1		3	4	5	5	8	5	3	6
AT5G47700.1	60S acidic ribosomal protein family						4	3		
AT2G32060.1	Ribosomal protein L7Ae/L30e/S12e/Gadd45				2	3			2	2
AT5G58250.1	unknown protein	5								
AT3G57240.1	beta-1,3-glucanase 3					6	6		3	
AT1G65930.1	cytosolic NADP+-dependent isocitrate dehydrogenase		4	5	5	10	12	10	7	8
AT2G05990.1	NAD(P)-binding Rossmann-fold superfamily protein	2	2	2	2					
AT1G20340.1	Cupredoxin superfamily protein		21	18	18	14	16			
AT4G33010.1	glycine decarboxylase P-protein 1	10	16	27	25	16	19	15	16	11
AT2G46820.1	photosystem I P subunit	5	5	5	2					
AT1G76180.1	Dehydrin family protein						9			
AT5G45775.1	Ribosomal L5P family protein				5	6	6	5	6	
AT2G01250.1	Ribosomal protein L30/L7 family protein				4	7	5	4	6	3
AT5G42270.1	FtsH extracellular protease family	12	16	7	6	4				
AT1G08830.1	copper/zinc superoxide dismutase 1					4	3			4
AT3G44100.1	MD-2-related lipid recognition domain									4
AT5G16710.1	dehydroascorbate reductase 1	6	4							
AT4G35450.3	ankyrin repeat-containing protein 2				4	7	5	5	3	
AT1G66410.1	calmodulin 4			2	5	4	5	5	3	
AT1G24020.1	MLP-like protein 423				2				2	
AT2G14610.1	pathogenesis-related gene 1					6	5	2		
AT5G08280.1	hydroxymethylbilane synthase	7	7	4	5	2				
AT3G52380.1	chloroplast RNA-binding protein 33	7	6	4	3					
AT3G14067.1	Subtilase family protein							5		12
AT2G24270.2	aldehyde dehydrogenase 11A3					4	5	4		
AT1G62780.1	unknown protein	5	4							
AT3G25530.2	glyoxylate reductase 1				3		6			
AT1G11430.1	plastid developmental protein DAG, putative	5	5	4						
AT1G75780.1	tubulin beta-1 chain			4	3	6	14	11	9	5
AT3G60770.1	Ribosomal protein S13/S15						5			
AT3G62870.1	Ribosomal protein L7Ae/L30e/S12e/Gadd45		10	7	12	6	12	4		
AT4G34670.1	Ribosomal protein S3Ae					4	6	5	5	
AT3G25920.1	ribosomal protein L15	9	7	4	4					
AT5G11420.1	Protein of unknown function, DUF642		2			8	12	4		
AT2G33040.1	gamma subunit of Mt ATP synthase			6	4	9	9	9	3	8
AT1G07770.1	ribosomal protein S15A					2	2		2	
AT1G66200.2	glutamine synthase clone F11	2	3	5	4		3			
AT1G09640.1	Translation elongation factor EF1B, gamma chain						8	5		
AT3G48930.1	Nucleic acid-binding, OB-fold-like protein			3	3	3	4	3	2	
AT2G18110.1	Translation elongation factor EF1B/ribosomal					3	4			4

AT5G30510.1	ribosomal protein S1	8	10	6	5	3				
AT5G01530.1	light harvesting complex photosystem II	9	9	8	9	7	5		5	4
AT1G09780.1	Phosphoglycerate mutase, 2,3-bisphosphoglycerate				4	4	9	3		
AT4G14880.1	O-acetylserine (thiol) lyase (OAS-TL) isoform A1			2	4	6	8	6	7	3
AT1G21750.2	PDI-like 1-1					6	7	7	6	3
AT3G54890.4	photosystem I light harvesting complex gene 1	4	6	5	5					
AT1G75040.1	pathogenesis-related gene 5			6	7	15	13	11	10	8
AT2G33800.1	Ribosomal protein S5 family protein	9	11	5	8	4	4			
AT5G56010.1	heat shock protein 81-3			3	4	7	17	9	8	6
AT3G61440.1	cysteine synthase C1			3		5	2	2		
AT5G56000.1	HEAT SHOCK PROTEIN 81.4		5	3	6	7	15	9	8	6
AT1G72370.2	40s ribosomal protein SA			4	4	7	9	4	6	2
AT2G30950.1	FtsH extracellular protease family	15	19	9	11	6				
AT1G55480.1	protein containing PDZ domain, a K-box domain	5	8	3		3				
AT5G16130.1	Ribosomal protein S7e family protein			2	3	2	6			
AT3G08580.1	ADP/ATP carrier 1					3	3	6	8	4
AT1G48830.1	Ribosomal protein S7e family protein						5			
AT1G05190.1	Ribosomal protein L6 family	2		2						
AT1G17290.1	alanine aminotransferas						4		4	4
AT2G42100.1	Actin-like ATPase superfamily protein						9			5
AT3G01480.1	cyclophilin 38	5	7	5	5	5				
AT3G15360.1	thioredoxin M-type 4	6	9	5						
AT3G55280.3	ribosomal protein L23AB			4	3					
AT1G20440.1	cold-regulated 47					3	7	5	4	
AT2G19730.1	Ribosomal L28e protein family									2
AT3G15730.1	phospholipase D alpha 1						6			2
AT1G20450.2	Dehydrin family protein						5		2	
AT1G74050.1	Ribosomal protein L6 family protein				3	5	6			
AT1G14320.1	Ribosomal protein L16p/L10e family protein			2	2	2	5		2	
AT5G15650.1	reversibly glycosylated polypeptide 2						5			
AT5G27850.1	Ribosomal protein L18e/L15 superfamily protein		2	4	3	2	4		4	
AT5G16390.2	chloroplastic acetylcoenzyme A carboxylase 1	7	6	6	5					
AT5G02790.1	Glutathione S-transferase family protein					4	2			
AT2G44120.1	Ribosomal protein L30/L7 family protein				3	7	4	4	3	
AT4G17530.1	RAB GTPase homolog 1C				2		4			
ATCG01120.1	chloroplast ribosomal protein S15			2						
AT5G45390.1	CLP protease P4	7	6	7	7					
AT3G53020.1	Ribosomal protein L24e family protein			2		3	3		3	
AT1G18080.1	Transducin/WD40 repeat-like superfamily protein			2	3	4	6	4	4	4
AT3G02730.1	thioredoxin F-type 1	4	5	3	3	3	2			
AT2G34480.1	Ribosomal protein L18ae/LX family protein						4			
AT5G25980.1	glucoside glucohydrolase 2	10	10	10	10	6	7	3	4	
AT4G15000.2	Ribosomal L27e protein family								2	
AT1G32990.1	plastid ribosomal protein l11	4	4	3	3					
AT2G26080.1	glycine decarboxylase P-protein 2	4	9	16	15	7	12	8	5	2

AT5G10360.2	Ribosomal protein S6e			2		2	2	4	4	6
AT5G17710.1	Co-chaperone GrpE family protein	11	10							
AT2G44060.1	Late embryogenesis abundant protein							5	3	
AT1G70310.1	spermidine synthase 2					2				
AT2G41530.1	S-formylglutathione hydrolase						4		3	
AT1G33120.1	Ribosomal protein L6 family								5	
AT3G10060.1	FKBP-like peptidyl-prolyl cis-trans isomerase	2	3							
AT2G47470.2	thioredoxin family protein					2				
AT1G52230.1	photosystem I subunit H2		6							
AT1G51980.1	Insulinase (Peptidase family M16) protein				3	4	6	5	3	
AT3G56910.1	plastid-specific 50S ribosomal protein 5		5							
AT5G45680.1	FK506-binding protein 13	5	5	2	2					
AT1G11840.2	glyoxalase I homolog					3	3	2		6
ATCG00680.1	photosystem II reaction center protein B	9	13		3				3	
AT2G03440.1	nodulin-related protein 1						3			
AT5G47210.1	Hyaluronan / mRNA binding family		3	4	5	4	3			
ATCG00065.1	ribosomal protein S12A	2								
AT1G74970.1	ribosomal protein S9		3		2					
AT5G01410.1	Aldolase-type TIM barrel family protein		5	5	7	4	5	4	4	3
AT3G54400.1	Eukaryotic aspartyl protease family protein					3	4			4
AT1G12840.1	vacuolar ATP synthase subunit C (VATC)				2	3		4	4	6
AT4G16720.1	Ribosomal protein L23/L15e family protein						3	3		
AT1G80380.3	P-loop containing nucleoside triphosphate hydrolases superfamily protein	2	5	2	4					
AT4G28660.1	photosystem II reaction center PSB28 protein	4	4							
AT3G24503.1	aldehyde dehydrogenase 2C4						4			
AT5G14780.1	formate dehydrogenase						2			
AT3G52300.1	ATP synthase D chain, mitochondrial								3	
AT5G18380.2	Ribosomal protein S5 domain 2-like superfamily protein						3			
AT1G78850.1	D-mannose binding lectin protein					4	5	5	3	
ATCG00270.1	photosystem II reaction center protein D	6	9		3					
AT3G02090.1	Insulinase (Peptidase family M16) protein					8	7	7		9
ATCG00800.1	structural constituent of ribosome			4						
AT2G21870.2	copper ion binding;cobalt ion binding;zinc ion binding			2		2	2	3	4	
AT1G11910.1	aspartic proteinase A1						4		3	12
AT5G44130.1	FASCICLIN-like arabinogalactan protein 13 precursor					6	5	4		
AT5G54270.1	light-harvesting chlorophyll B-binding protein 3						2			
AT4G27520.1	early nodulin-like protein 2					7	3			
AT5G20010.1	RAS-related nuclear protein-1					5	3			5
AT2G31390.1	pfkB-like carbohydrate kinase family protein						4			
AT2G24020.2	Uncharacterised BCR, YbaB family COG0718	5	6	3	4					
AT4G29060.1	elongation factor Ts family protein	12	13	11	10	3				
AT4G01050.1	thylakoid rhodanese-like	5	6		2					
AT3G46490.1	2-oxoglutarate (2OG) and Fe(II)-dependent oxygenase superfamily protein			2						
AT1G63940.4	monodehydroascorbate reductase 6	6	4	5	5		3		4	
AT4G16830.2	Hyaluronan / mRNA binding family					2				

AT3G08030.2	Protein of unknown function, DUF642						3			
AT5G02240.1	NAD(P)-binding Rossmann-fold superfamily protein		3		5	6				4
AT3G08940.1	light harvesting complex photosystem II	4	3		3	3				
AT1G71500.1	Rieske (2Fe-2S) domain-containing protein		4							
ATCG00280.1	photosystem II reaction center protein C	6	10			4			3	
AT4G21210.2	PPDK regulatory protein		2							
AT2G37270.1	ribosomal protein 5B					2				
AT3G46970.1	alpha-glucan phosphorylase 2					5	8	5	3	
AT1G44575.1	Chlorophyll A-B binding family protein		2							
AT4G12800.1	photosystem I subunit l	4	3	2	3	2				
AT1G78380.1	glutathione S-transferase TAU 19				3					
AT5G13510.1	Ribosomal protein L10 family protein		2							
AT4G02450.2	HSP20-like chaperones superfamily protein					3				
AT3G15190.1	chloroplast 30S ribosomal protein S20, putative	4	3	3						
AT1G78830.1	Curculin-like (mannose-binding) lectin family protein					4				
AT3G14310.1	pectin methylesterase 3					6	4	3		5
AT5G25460.1	Protein of unknown function, DUF642					5	8	2		
AT5G50850.1	Transketolase family protein				2	4	5			
AT1G74470.1	Pyridine nucleotide-disulphide oxidoreductase	4	2							
AT4G24190.1	Chaperone protein htpG family protein					5	8	8	7	
AT1G47128.1	Granulin repeat cysteine protease family protein					7	9	9	7	15
AT5G48300.1	ADP glucose pyrophosphorylase 1	6	7	7	3	4	3			3
AT4G31990.4	aspartate aminotransferase 5		2	4						
AT1G35680.1	Ribosomal protein L21	3								
AT4G13930.1	serine hydroxymethyltransferase 4					4	4	4	5	4
AT5G23900.1	Ribosomal protein L13e family protein						3			
AT3G10920.2	manganese superoxide dismutase 1	2	3							
AT4G35830.1	aconitase 1		5	5	3	5	11			5
AT5G20890.1	TCP-1/cpn60 chaperonin family protein								4	
AT1G29660.1	GDSL-like Lipase/Acylhydrolase superfamily protein				3	8	5			
AT3G25770.1	allene oxide cyclase 2	2								
AT5G11670.1	NADP-malic enzyme 2					5	4	6	4	6
AT3G23990.1	heat shock protein 60					4	5		3	
AT1G69740.1	Aldolase superfamily protein	2								
AT3G58610.1	ketol-acid reductoisomerase		3	4	3					
AT4G09010.1	ascorbate peroxidase 4		2							
AT3G16530.1	Legume lectin family protein						5	3		
AT2G20140.1	AAA-type ATPase family protein							2		
AT4G12720.1	MutT/nudix family protein				6					
AT3G09840.1	cell division cycle 48		2			4	3	4	4	
AT5G63310.1	nucleoside diphosphate kinase 2	2			2					
AT3G57680.1	Peptidase S41 family protein				2					
AT5G58290.1	regulatory particle triple-A ATPase 3						4			
AT2G37700.1	Fatty acid hydroxylase superfamily								2	
AT1G71980.1	Protease-associated (PA) RING/U-box zinc finger family protein			2						

AT1G16905.1	Curculin-like (mannose-binding) lectin family protein						2			
AT2G05710.1	aconitase 3			3	2	3	5			3
AT3G15356.1	Legume lectin family protein					3	5			
AT5G03350.1	Legume lectin family protein					2	5			2
AT1G65260.1	plastid transcriptionally active 4		2							
AT3G25860.1	2-oxoacid dehydrogenases acyltransferase family				3					
AT3G20820.1	Leucine-rich repeat (LRR) family protein						4			
AT3G18490.1	Eukaryotic aspartyl protease family protein					3	3			
AT5G28840.1	GDP-D-mannose 3',5'-epimerase				2	3	5			
AT5G46420.1	16S rRNA processing protein RimM family			2						
AT1G76160.1	SKU5 similar 5						3			
AT3G08590.1	Phosphoglycerate mutase, 2,3-bisphosphoglycerate-independent						2			
AT5G67360.1	Subtilase family protein					3				
AT4G25130.1	peptide met sulfoxide reductase 4		3							
AT4G27440.1	protochlorophyllide oxidoreductase B		2							
AT2G18969.1	unknown protein	3								
AT5G57590.1	adenosylmethionine-8-amino-7-oxononanoate			4						
AT2G15620.1	nitrite reductase 1		3							
AT1G70730.1	Phosphoglucomutase/phosphomannomutase								2	
AT5G53480.1	ARM repeat superfamily protein						4			
AT5G51820.1	phosphoglucomutase	2	2							
AT3G19170.2	presequence protease 1				4					
AT2G03667.1	Asparagine synthase family protein						2			
AT3G29360.1	UDP-glucose 6-dehydrogenase family protein						3			
AT1G77510.1	PDI-like 1-2					2		3		
AT1G09750.1	Eukaryotic aspartyl protease family protein						4	3		
AT2G41220.1	glutamate synthase 2	3	6	7	5	5	4	3		
AT1G51850.1	Leucine-rich repeat protein kinase family protein				2					
AT4G31480.1	Coatomer, beta subunit					2				
AT2G42600.2	phosphoenolpyruvate carboxylase 2						4			
AT1G79600.1	Protein kinase superfamily protein		3							
AT5G43740.1	Disease resistance protein (CC-NBS-LRR class)			2						
AT4G37910.1	mitochondrial heat shock protein 70-1							4	3	
AT3G52500.1	Eukaryotic aspartyl protease family protein								2	
AT1G52315.1	Regulator of Vps4 activity in the MVB pathway		3							
AT3G48860.1	unknown protein	2								
AT5G42870.2	phosphatidic acid phosphohydrolase 2		2							
AT3G01780.1	ARM repeat superfamily protein					2				
AT5G24120.1	sigma factor E						3			
AT1G49630.1	presequence protease 2			3	3	3				
AT5G11390.1	WPP domain-interacting protein 1			2						
AT3G59970.3	methylenetetrahydrofolate reductase 1							2		
AT3G19100.1	Protein kinase superfamily protein					3				
AT4G26970.1	aconitase 2				2		3		3	
AT4G16155.1	dihydrolipoyl dehydrogenases	2								
AT1G16300.1	glyceraldehyde-3-phosphate dehydrogenase				4	3				

AT5G45340.2	cytochrome P450, family 707, subfamily A, polypeptide 3		2		2				
AT1G50480.1	10-formyltetrahydrofolate synthetase						3		
AT5G16020.1	gamete-expressed 3						2		
AT2G37800.1	Cysteine/Histidine-rich C1 domain family protein						3		
AT2G20290.1	myosin-like protein XIG					2			
AT3G14570.2	glucan synthase-like 4		2						
AT4G14605.1	Mitochondrial transcription termination factor		3						
AT2G28540.2	RNA binding (RRM/RBD/RNP motifs) family		2				2		
AT4G20430.2	Subtilase family protein							3	
AT1G35730.1	pumilio 9	2							
AT1G01320.2	Tetratricopeptide repeat (TPR)-like						4		
AT3G20250.1	pumilio 5						3		
AT3G61570.1	GRIP-related ARF-binding domain-containing protein		2						
AT5G43810.1	Stabilizer of iron transporter SufD		2	3					
AT5G60410.3	DNA-binding protein with MIZ/SP-RING					2			
AT1G12800.1	Nucleic acid-binding, OB-fold-like protein					2			
AT1G42440.1	unknown protein	2							
AT4G23160.1	cysteine-rich RLK					3	3		
AT1G80070.1	Pre-mRNA-processing-splicing factor				3	2	2	4	3
AT1G17580.1	myosin 1			2					
AT1G03060.1	Beige/BEACH domain ;WD domain	2							
AT1G08840.1	DNA replication helicase, putative					2			
AT5G05560.1	E3 ubiquitin ligase, putative				2				
AT1G20960.1	U5 small nuclear ribonucleoprotein helicase						2	2	
AT2G35630.1	ARM repeat superfamily protein				2				
AT2G17930.1	Phosphatidylinositol 3- and 4-kinase family protein		3			2			
AT5G23110.1	Zinc finger, C3HC4 type (RING finger)					2			

Table A.2: 188 protein groups in *Medicago truncatula*

Accession number	Protein description	PSM1	PSM2	PSM3	PSM4	PSM5	PSM6	PSM9
G8A318	ATP synthase subunit beta	103	118	90	42	47	34	58
TC194452	ATP synthase CF1 alpha subunit	32	36	33	25	28	23	31
TC180562	Phosphoglycerate kinase	49	70	33	31	21	22	28
G7IT85	Phosphoglycerate kinase	48	70	35	28	17	20	27
G7JGC9	Low-temperature inducible		17	5				5
TC173680	H+-transporting two-sector ATPase, alpha/beta subunit	195	244	166	64	76	55	101
TC198638	similar to UniRef100_A7PIQ8 Cluster	87	115	50	20	35	26	48
G7K2D0	Photosystem I reaction center subunit II	8	20	6		5		10
TC195737	Photosystem I reaction center subunit IV	7	9	4		7	5	
CX526357	homologue to UniRef100_Q7Q7K6 Cluster		6					
B7FJ16	Putative uncharacterized protein	23	36	23	14	15	12	19
G7ZVI4	Oxygen-evolving enhancer protein	45	59	32	20	21	13	21
TC173939	Glyceraldehyde-3-phosphate dehydrogenase	19	19	22	16	10	11	13
TC186274	Uncharacterized protein	8	13					
C8CGU0	Putative glyceraldehyde-3-phosphate dehydrogenase	53	70	43	34	26	38	36
G8D4Z4	Ribulose bisphosphate carboxylase large chain	171	70	52	29	32	22	26
TC195144	Plastocyanin	29	40	28	12	14	11	22
G0WYY8	Ribulose bisphosphate carboxylase large chain	192	84	61	25	38	27	39
TC198514	Phosphoribulokinase	19	40	7	2	8	2	9
G7JAX5	Actin		16	6				
G7J5Y4	Glyceraldehyde-3-phosphate dehydrogenase	32	49	21	9	5	7	14
G7JW95	Ferredoxin-NADP reductase	26	24	10		3		5
G7JG19	Ribulose bisphosphate carboxylase large	428	211	154	101	111	93	103
TC173782	Glycolate oxidase	21	30	14				
G7KMR3	Ribulose bisphosphate carboxylase small chain	61	71	38	13	9	7	20
TC188747	Glycine cleavage system H protein	9	18	4	8	8	5	15
G7IF28	Transketolase	30	41	30	14	12	13	32
B7FHB2	Ribulose bisphosphate carboxylase small chain	53	62	34	11	7	7	17
TC183950	RuBisCO large subunit-binding protein subunit beta	5	11	5				
TC181859	Ribulose bisphosphate carboxylase small chain 3A	39	55	30	12	12	7	20
TC198054	Ribulose bisphosphate carboxylase small chain	39	52	28	11	8	7	19
TC174573	Aminomethyltransferase, mitochondrial	5	23	3		2		8
TC172860	Ribulose bisphosphate carboxylase	331	185	129	92	107	89	93
TC179581	RuBisCO large subunit-binding protein subunit beta	13	29	13	8			4
TC186736	AAA ATPase	45	68	28	13	13	15	22
TC173920	Triosephosphate isomerase		9	5				

TC184208	RNA-binding region RNP-1	4	11	6		2		
TC182071	Transketolase	28	43	29	13	16	16	32
B7FIL9	Fructose-bisphosphate aldolase	33	43	25	3	10		16
G7JQB5	ATP synthase subunit alpha	63	68	38	26	23	23	31
B7FIH3	Putative uncharacterized protein		19	4				
TC175230	RuBisCO large subunit-binding protein subunit alpha	11	31					10
TC196303	Oxygen-evolving enhancer protein	26	34	17		2		9
G7J486	Elongation factor Tu	24	26	11				
TC174754	Peroxiredoxin Q, chloroplast precursor		12					
G7IE32	2-Cys peroxiredoxin BAS1	8	12	4				4
TC180056	ATP synthase subunit beta	7	17	12	6	5	5	8
TC192637	similar to UniRef100_A7NYJ8 Cluster	4	9					
TC183313	50S ribosomal protein L12-3	4	13					
DY615543	Granulin							5
TC186757	similar to UniRef100_A7PCN3 Cluster	11	15	9	9	8	6	11
TC195765	Inorganic pyrophosphatase_rframe2	4	3					
B7FHF6	Putative uncharacterized protein		7					
TC185701	Serine-hydroxymethyltransferase	11	15	8		5		7
G7IJ45	Photosystem II 10 kDa polypeptide	13	12	10				
TC174211	2-Cys peroxiredoxin	9	12	4				4
TC174160	Uncharacterized protein	3	14					
TC192151	Ribulose bisphosphate carboxylase/oxygenase activase	43	67	31	15	11	11	28
G7JAI2	ATP synthase	4	4					
A9YWS0	Serine hydroxymethyltransferase	12	16	7		5		6
TC182323	RuBisCO large subunit-binding protein subunit beta	8	20					
TC184082	similar to UniRef100_A7PDS7 Cluster	9	14					3
TC194222	Harpin binding protein		6				3	
G7K9H5	Oxygen evolving enhancer protein	24	40	18	8	12	8	10
G7JLC6	ATP synthase	6	13					
Q84UC1	Glutamine synthetase	18	20	10	2	5	2	4
G7J2H2	Glyceraldehyde 3-phosphate dehydrogenase	6	5	7	5			4
TC174569	Thioredoxin M-type	5	13	4				
TC183731	Carbonic anhydrase		6					
TC173105	Phosphoglycerate kinase	13	11	7	4	4		6
G8A0S6	Cytosolic fructose-1 6-bisphosphatase		4					
TC178655	similar to UniRef100_Q08883	3				3	2	8
TC178815	similar to UniRef100_Q08883					3	3	
O48904	Malate dehydrogenase		9					
AL381994	Acid phosphatase							

TC181180	Nucleoside diphosphate kinase 1		4					
EY478847	homologue to UniRef100_Q9XI93		5					
TC184150	ATP synthase CF1 alpha subunit;	16	19	11	13	6	9	7
G7K4T4	Fructose-bisphosphate aldolase		3					
TC180857	Ribosomal protein L1		7					
TC191548	Ribonuclease HII							
Q1SKX2	Chaperone DnaK	13	31					
TC180688	Non-specific lipid-transfer protein precursor		6	6		3		
G7JSV9	Ubiquitin		5					
TC175118	similar to UniRef100_A7QWX5 Cluster		6					
G7JAP0	Sedoheptulose-1 7-bisphosphatase	12	21	6				3
G7K0Q6	Chlorophyll a-b binding protein	11	13	5				
TC182098	ATP synthase gamma chain	8	10	3				
TC176560	Uncharacterized protein		3					
TC176326	Malate dehydrogenase	5	13					
B7FIY3	14-3-3 protein		3					
Q2HT97	Heat shock protein Hsp70		8					
B7FHW7	Putative uncharacterized protein	3	7					
BQ152514	Photosystem II reaction center PSB28 protein		4					
G7L1U4	Chloroplast ribose-5-phosphate isomerase		12					
TC184797	glutathione S-transferase							
B7FGU7	Cytochrome b6-f complex iron-sulfur subunit	8	14	5				3
TC174775	Enolase							
TC187948	Peptidyl-prolyl cis-trans isomerase			2				
G7JYY7	Alanine aminotransferase	4	6					
G7K6C4	Putative uncharacterized protein		4					
Q84RD8	Adenosylhomocysteinase			5	4		3	5
G7J013	Alanine glyoxylate aminotransferase	4						
B7FME3	Putative uncharacterized protein	7	7	6		4		
G7IED1	MRNA-binding protein	9	14					
TC175955	similar to UniRef100_A7PVK1 Cluster		10					
CX520563	Uncharacterized protein	5	4					
CX525843	Elongation factor 1-alpha		6					
TC180095	Photosystem II type I chlorophyll a/b-binding protein	5	6	5				
G7JE46	Thylakoid lumenal 16.5 kDa protein		3					
EX530142	Actin		6					
DY616891	similar to UniRef100_A7LNX7		3					
Q84RD9	Adenosylhomocysteinase			3	5		3	4
G7KFV1	UTP-glucose 1 phosphate uridylyltransferase							

B7FKR3	Putative uncharacterized protein	3	3					
G7KN61	Elongation factor 1-alpha	7	12	6				6
TC175661	Triosephosphate isomerase		5					
G7IL22	Putative uncharacterized protein		13					
TC178805	Glycine							
TC187801	Dihydrolipoyl dehydrogenase		4					
EV254789	S-adenosylmethionine synthetase							
TC173159	UDP-glucose pyrophosphorylase							
ES612239	homologue to UniRef100_UPI0001596BB1 Cluster	2						
TC175690	Hydroxypyruvate reductase	2	3					
B7FJ57	Peptidyl-prolyl cis-trans isomerase		2					
TC192287	similar to UniRef100_A7NYV0 Cluster		2					
EV262290	similar to UniRef100_A7PPK6 Cluster		4					
G7L2M8	GrpE protein homolog		5					
TC192982	Malate dehydrogenase		4					
TC178104	homologue to UniRef100_P31165 Cluster		5					
G7KAG7	Putative uncharacterized protein		6					
B7FHD5	Putative uncharacterized protein		4					
B7FI72	Ribosome-recycling factor		6					
TC197566	similar to UniRef100_A7PJ10 Cluster		4					
TC177592	Catalase							
TC192478	Dihydrolipoyl dehydrogenase		4	4				
G7JG73	Glycine-rich RNA binding protein							
TC181439	homologue to UniRef100_Q9XQB4 Cluster	4						
TC180407	similar to UniRef100_Q41016 Cluster		4					
B7FN63	Photosystem I reaction center subunit VI		5					
TC194267	Histone H2A		4					
G4W9I5	Glutamate 1-semialdehyde aminotransferase		5					
Q40365	Peroxidase							8
G7IK85	Magnesium-chelatase subunit chlI		4					
G7L0I8	Methionine synthase							2
TC179289	Ferritin-2, chloroplast precursor		4					
A6Y950	Vacuolar H+-ATPase B subunit							
G7K694	Fructose-bisphosphate aldolase	3	3					
B7FHZ5	Putative uncharacterized protein	10	7	5				
O81391	Chlorophyll a/b binding protein	13	12	9	4	5	3	3
G7I9Z0	Glycine dehydrogenase P	6	7	3				7
G7I9Q9	ATP synthase subunit alpha	6	4					
B7FJL0	Putative uncharacterized protein	2						

CX525630	homologue to UniRef100_Q1HRU0 Cluster		2	
Q8W596	Superoxide dismutase		3	
TC195187	homologue to UniRef100_Q43437 Cluster	7	6	5
TC175890	similar to UniRef100_A7P8V3 Cluster		3	
B7FK19	Putative uncharacterized			
TC173971	similar to UniRef100_Q7X9F7 Cluster			
B7FIL0	Putative uncharacterized protein			
G7KY52	Elongation factor P		2	
TC193088	similar to UniRef100_A7LNX7 Cluster		2	
G7JNN9	Cysteine synthase		3	
B7FK62	Putative uncharacterized protein	2	3	
G7I8D4	Thioredoxin H-type 5		3	
Q45FF2	Pyridoxal biosynthesis protein PDX1.3			
TC178298	homologue to UniRef100_A7PCK8		4	
TC174430	similar to UniRef100_A7PNN9 Cluster		4	
TC182259	Vacuolar ATP synthase catalytic subunit A			
TC174997	Monodehydroascorbate reductase			
TC185800	Fructose-1,6-bisphosphatase	3	6	
TC183128	Chloroplast pigment-binding protein		2	
B7FHI6	Putative uncharacterized protein		3	
B7FIJ7	Putative uncharacterized protein			
B7FKG8	Putative uncharacterized protein		4	
G7JTH6	Caffeic acid 3-O-methyltransferase			
B7FJ10	Putative uncharacterized protein		3	
TC189512	homologue to UniRef100_A7NWY2 Cluster			
G7JL79	Ferredoxin-nitrite reductase		4	
TC187551	Ferredoxin-dependent glutamate synthase	14	9	
G7ITZ5	Aconitate hydratase			
G7IH13	Elongation factor EF-2			
G7LIT0	ATP-dependent Clp protease ATP-binding subunit	6	5	
G7JQC5	Photosystem II D2 protein			
G7KEK9	Glucose-1-phosphate adenylyltransferase		3	
G7I682	Putative uncharacterized protein		2	
A2Q199	Chaperone Dank		3	

Table A.3: Isolated chloroplast proteins from Medicago truncatula leaves using Percoll density gradients. In total 38 different proteins were found.

Accession number	Protein description	spectral counts
G8A318	ATP synthase subunit beta	153
TC194452	ATP synthase CF1 alpha subunit	27
G7ZVI4	Oxygen-evolving enhancer protein	58
TC195144	Plastocyanin	116
TC180562	Phosphoglycerate kinase	49
B7FJ16	Putative uncharacterized protein	26
G7KMR3	Ribulose bisphosphate carboxylase small chain	32
B7FHB2	Ribulose bisphosphate carboxylase small chain	25
B7FMC2	Ribulose bisphosphate carboxylase small chain	21
C8CGU0	Putative glyceraldehyde-3-phosphate dehydrogenase	53
TC181859	Ribulose bisphosphate carboxylase small chain 3A	20
G7JG19	Ribulose bisphosphate carboxylase large chain	997
G7JML2	Glyceraldehyde-3-phosphate dehydrogenase	19
TC198638	similar to UniRef100_A7PIQ8 Cluster	61
G7JZW8	Glycine cleavage system H protein	10
B7FHT0	Putative uncharacterized protein	17
G7JQB5	ATP synthase subunit alpha	34
G7K882	Phosphoribulokinase	25
TC174775	Enolase	5
TC180858	Fructose-bisphosphate aldolase 1, chloroplast precursor	11
TC178815	Narbonin	5
G7JW95	Ferredoxin-NADP reductase	13
G7K2D0	Photosystem I reaction center subunit II	11
G7IF28	Transketolase	22
Q84UC1	Glutamine synthetase	18
TC186898	Elongation factor Tu	5
O81391	Chlorophyll a/b binding protein	4
TC186274	Uncharacterized protein	4
G7I4U4	Harpin binding protein	4
TC184150	ATP synthase CF1 alpha subunit	9
B7FIL9	Fructose-bisphosphate aldolase	13
TC186757	similar to UniRef100_A7PCN3	4
G7JJ97	Aminomethyltransferase	4
G7ZUV5	2-cys peroxiredoxin	3
TC196303	Oxygen-evolving enhancer protein	7
G7IAW2	ATP synthase subunit beta	8
TC186276	Chaperone Dank	3

Table A.4. The tripole quadrupole tune settings for the native peptides and the heavy labeled peptides are shown.

precursor ion (m/z)	product ion (m/z)	collision energy	peptide	name
852.738225	744.388644	34.7	NNAGFPHNVIFDEDEIPSGVDAAK	Medtr_Chl1
852.738225	647.335881	34.7	NNAGFPHNVIFDEDEIPSGVDAAK	Medtr_Chl1
852.738225	404.213974	34.7	NNAGFPHNVIFDEDEIPSGVDAAK	Medtr_Chl1
855.409624	752.402843	34.7	NNAGFPHNVIFDEDEIPSGVDAA[Lys(13C6; 15N2)]	Medtr_Chl1
855.409624	655.35008	34.7	NNAGFPHNVIFDEDEIPSGVDAA[Lys(13C6; 15N2)]	Medtr_Chl1
855.409624	412.228173	34.7	NNAGFPHNVIFDEDEIPSGVDAA[Lys(13C6; 15N2)]	Medtr_Chl1
589.834652	966.509551	20.4	LVNE[Leu(13C6;15N9)]TEFA[Lys(13C6; 15N2)]	Medtr_Chl1
589.834652	723.42403	20.4	LVNE[Leu(13C6;15N9)]TEFA[Lys(13C6; 15N2)]	Medtr_Chl1
589.834652	603.322802	20.4	LVNE[Leu(13C6;15N9)]TEFA[Lys(13C6; 15N2)]	Medtr_Chl1
529.766905	773.378808	18.8	WVDALSDPR	Medtr_VaPe1
529.766905	272.171716	18.8	WVDALSDPR	Medtr_VaPe1
529.766905	286.155003	18.8	WVDALSDPR	Medtr_VaPe1
534.77104	783.387077	18.8	WVDALSDP[Arg(13C6; 15N4)]	Medtr_VaPe1
534.77104	282.179985	18.8	WVDALSDP[Arg(13C6; 15N4)]	Medtr_VaPe1
534.77104	286.155003	18.8	WVDALSDP[Arg(13C6; 15N4)]	Medtr_VaPe1
810.940847	1333.747427	27.2	TWPEDIIPLQPVGR	Medtr_VaPe1
810.940847	879.541063	27.2	TWPEDIIPLQPVGR	Medtr_VaPe1
810.940847	766.456999	27.2	TWPEDIIPLQPVGR	Medtr_VaPe1
815.944982	1343.755696	27.2	TWPEDIIPLQPVG[Arg(13C6; 15N4)]	Medtr_VaPe1
815.944982	889.549332	27.2	TWPEDIIPLQPVG[Arg(13C6; 15N4)]	Medtr_VaPe1
815.944982	776.465268	27.2	TWPEDIIPLQPVG[Arg(13C6; 15N4)]	Medtr_VaPe1
587.831102	962.502451	20.4	LVNE[Leu(13C6;15N)]TEF[Ala(13C3;15N)]K	Medtr_VaPe1
587.831102	848.459523	20.4	LVNE[Leu(13C6;15N)]TEF[Ala(13C3;15N)]K	Medtr_VaPe1
587.831102	719.41693	20.4	LVNE[Leu(13C6;15N)]TEF[Ala(13C3;15N)]K	Medtr_VaPe1
838.951275	991.530617	28.1	VGTLDSLLSLSDDLTK	Medtr_VaPe2
838.951275	878.446553	28.1	VGTLDSLLSLSDDLTK	Medtr_VaPe2
838.951275	886.488024	28.1	VGTLDSLLSLSDDLTK	Medtr_VaPe2
842.958374	999.544816	28.1	VGTLDSLLSLSDDLT[Lys(13C6;15N2)]	Medtr_VaPe2
842.958374	886.460752	28.1	VGTLDSLLSLSDDLT[Lys(13C6;15N2)]	Medtr_VaPe2
842.958374	886.488024	28.1	VGTLDSLLSLSDDLT[Lys(13C6;15N2)]	Medtr_VaPe2
587.329425	955.485287	20.4	L[Val(13C5; 15N)]NELTEF[Ala(13C3;15N)]K	Medtr_VaPe2
587.329425	841.442359	20.4	L[Val(13C5; 15N)]NELTEF[Ala(13C3;15N)]K	Medtr_VaPe2
587.329425	712.399766	20.4	L[Val(13C5; 15N)]NELTEF[Ala(13C3;15N)]K	Medtr_VaPe2
877.45759	1040.548333	29.2	GDEVVTIENLANVQPR	Medtr_Mito2
877.45759	684.378748	29.2	GDEVVTIENLANVQPR	Medtr_Mito2
877.45759	613.341635	29.2	GDEVVTIENLANVQPR	Medtr_Mito2
882.461724	1050.556602	29.2	GDEVVTIENLANVQP[Arg(13C6;15N4)]	Medtr_Mito2
882.461724	694.387017	29.2	GDEVVTIENLANVQP[Arg(13C6;15N4)]	Medtr_Mito2
882.461724	623.349904	29.2	GDEVVTIENLANVQP[Arg(13C6;15N4)]	Medtr_Mito2
529.784038	846.408323	18.7	LVNETEFA[Lys(13C6; 15N2)]	Medtr_Mito2
529.784038	603.322802	18.7	LVNETEFA[Lys(13C6; 15N2)]	Medtr_Mito2
529.784038	373.23253	18.7	LVNETEFA[Lys(13C6; 15N2)]	Medtr_Mito2

Curriculum Vitae

Benedict Dirnberger;
Email: a0406970@unet.univie.ac.at
Tel: +43 699 10776153

Geboren.22.4.1984 in Wien

Ausbildung:

2000 – 2003	Lehre im Botanischen Garten der Universität Wien
2004	Berufsreifeprüfung (Externistenmatura)
10/2004	Studium der Biologie an der Universität Wien
	2. Studienabschnitt Genetik/Mikrobiologie

Diplomarbeit:

03/2012 ff	Dr. Stefanie Wienkoop und Prof. Dr. Wolfram Weckwerth: Department für Molekulare Systembiologie, Universität Wien: "A Subcellular Fractionation That Allows The Measurement Of The Proteome And The Metabolome"

Praktika:

04/2010:	Prof Schmetterer: Institut für physikalische Chemie, Universität Wien: „Studies of the glucose transporters in the cyanobacterium *Synechocystis"*
07/2010:	Prof. Bachmair :Max Ferdinand Perutz-Laboratories, Universität Wien: „Characterization of PHO2 Family of Ubiquitin-Conjugating Enzymes which are Involved in Programmed Cell Death in *Arabidopsis thaliana"*
03/2011	Laborarbeit zu verschieden Themen in der Abteilung Chromosomenbiologie, Universität Wien: „Meiotic chromosome behavior in the absence of the gene *SPO11* and the function of elongating the micronucleus in *Tetrahymena"* "Characterization of meiotic DNA double-strand breaks (DSBs) in wild type and of two mutants mnd1Δ and mms21Δ in *S.cerevisiae "* "Meiotic chromosome pairing in *Caenorhabditis elegans* wild- type and in two mutant strains:syp-2Δ and sun-1Δ"
07-8/2011:	Praxis Max Ferdinand Perutz-Laboratories, Universität Wien "A proteome- wide identification of kinase- substrate network in DNA damage response in *Arabidopsis thaliana"*

Auslandsaufenthalte:

7-8/2007:	Summer University of Bristol (UK)
7/2009:	Science Summer University of Cambridge (Uk)